NACA RM E54J01

NACA

RESEARCH MEMORANDUM

A STUDY OF FLAME-HOLDER ELEMENTS FOR USE IN HIGH-VELOCITY AFTERBURNERS

By Earl William Conrad, Wallace W. Velie, and Frederick W. Schulze

Lewis Flight Propulsion Laboratory
Cleveland, Ohio

NATIONAL ADVISORY COMMITTEE
FOR AERONAUTICS
WASHINGTON

February 23, 1955
Declassified September 1, 1961

59

NACA RM E54J01

NATIONAL ADVISORY COMMITTEE FOR AERONAUTICS

RESEARCH MEMORANDUM

A STUDY OF FLAME-HOLDER ELEMENTS FOR USE IN HIGH-VELOCITY AFTERBURNERS

By E. William Conrad, W. W. Velie, and Frederick W. Schulze

SUMMARY

A total of 31 flame-holder elements which could be classified into 7 distinct types was investigated under simulated afterburner operating conditions to determine their merit and feasibility for use in a high-velocity gas stream. Only the relative performance of the elements was determined inasmuch as the experimental technique did not provide absolute values. It did, however, allow the study of 12 flame-holder elements simultaneously. Fuel-air ratios varied between 0.023 and 0.0695. The total temperature at the burner inlet was set at 1250° F.

A V-gutter incorporating Inconel screening of varying densities exceeded the stability limits of the same size conventional V-gutter at fuel-air ratios below about 0.045. The blow-out limits of the screen-type flame holders were, however, sensitive to fuel-air ratio in contrast to the conventional V-gutter which proved fairly insensitive to fuel-air ratio. Other types of gutters which provided flame-immersed metal resulted in small benefits to stability at the high fuel-air ratios.

INTRODUCTION

Objective

Design studies of turbojet engines for supersonic propulsion (ref. 1, for example) have shown that substantial performance gains are possible by increasing the mass flow of air per unit of engine frontal area. Recent work with transonic compressors has shown that high unit mass flow rates are possible with good efficiency; however, the full advantage of this development cannot be exploited unless good combustion efficiency at high velocity levels can be achieved in both the main engine combustor and the afterburner. Investigations of main engine combustors designed for operation at high velocity are being conducted and preliminary data are contained in reference 2.

Considerations of the trends in air flow and engine pressure ratio together with the effect of velocity on momentum pressure drop in an

afterburner indicate that a reasonable compromise would be an average velocity of about 600 feet per second at the flame holder. This velocity is 40 or 50 percent higher than current practice and, on the basis of the present "state of the art," will be a major obstacle to the attainment of suitable afterburner operation. The attainment of satisfactory afterburner operation at a bulk velocity of 600 feet per second will probably require new information in all of the following areas:

(a) flame-holder blow-out limits - to allow higher velocities

(b) flame-holder pressure drop - particularly important in high-velocity afterburners because momentum pressure drop will also be high

(c) diffuser aerodynamics - to provide the flat velocity profile needed at the flame holder and thereby avoid extreme local velocities

(d) mixing techniques - to improve apparent flame propagation rate and thereby achieve good combustion efficiency in an afterburner of reasonable length

The brief study discussed herein comprises the first phase of a program on afterburning at high velocity and is concerned only with the experimental determination of the blow-out limits of various flame holders which embody various design philosophies. The direct objective was to find the type or types of flame holder having suitable stability limits for further use in connection with the studies of items (b), (c), and (d).

Test Technique

The technique used was aimed at the testing of several flame-holder designs simultaneously. This was done by utilizing full-scale flame-holder elements, but not complete flame holders. As shown by the sketches of figure 1, an element is representative of the geometry of a complete flame holder insofar as the aerodynamic and thermodynamic aspects are concerned, but may be arranged in several ways to form a complete flame holder. For example, figure 1 shows V-gutters in either a conventional or a lock-washer arrangement. The various flame-holder elements tested were mounted radially on a common cylinder as shown by the photographs of figure 2. Twelve such elements, each of different type or detailed construction were combined into a single test assembly, thus allowing the study of several designs simultaneously. The large economy in both facility running time and in fabrication time, compared to the use of complete flame holders, facilitated the study of entirely unconventional concepts which had little or no previous evidence of being suitable.

Inasmuch as the blow-out limit was the main point of interest in this phase of the program, the relative merit of the elements was determined by increasing the velocity and decreasing the pressure (at constant mass flow) until blow-out of all of the elements had occurred. The average velocity and pressure at which each element blew out is taken as a measure of its merit for comparison with the other elements. Repeated runs of this type were made at several constant values of mass flow and fuel-air ratio. Pressure was varied from about 26 to 5.2 inches of mercury absolute, and burner inlet bulk velocity was varied from approximately 200 to 1225 feet per second. In all, 31 different designs comprising 7 basic types were studied. A conventional V-gutter element was included in all test assemblies to provide a convenient reference level in considering the relative stability of elements in a given assembly.

INSTALLATION

The investigation was run in a burner rig as shown in figure 3. The flame holder was mounted in the $25\frac{3}{4}$-inch-diameter straight pipe section which was supplied with a vitiated gas stream preheated to 1250° F. The gas was preheated in 8 can-type combustors and then passed through a mixing chamber to assure a reasonably uniform temperature distribution entering the burner section. The air flow was set at a choked station upstream of the rig. A butterfly valve was provided downstream of the rig to allow control of exhaust pressure and thus burner inlet velocity and pressure (inlet pressure and velocity could not be controlled independently at one air flow). Fuel was admitted 31 inches upstream of the flame holder and initial ignition of the fuel was accomplished by use of a torch-type ignitor placed 14 inches upstream of the flame holder (the ignitor was extinguished after ignition occurred at the flame holder). The fuel injection system consisted of 24 spray bars equally spaced about the burner circumference and spraying upstream. Each bar had six 0.20-inch-diameter spray orifices, the spacing of which was based on seven areas of equal mass flow (fuel was deleted from the outer area to eliminate excessive shell heating). The pattern of orifices is shown in figure 4.

Two quartz windows placed slightly downstream of the flame holder (as shown in fig. 3) were provided for observation of the flame holder during combustion. Instrumentation included total-pressure rakes, thermocouple rakes, and static wall taps for measurement of burner inlet pressure and inlet temperature and computation of inlet velocity. The airflow measuring station was at a section immediately upstream of the preheater. Preheater and afterburner fuel flows were measured with fuel rotameters.

PROCEDURE

The stability limits of various prototype flame-holding elements mounted on a common support were observed and recorded. With the test assembly installed, runs were made at specifically set conditions of constant air flow and fuel-air ratio. After all flame-holding elements were observed to be supporting combustion, burner inlet pressure was reduced and inlet velocity simultaneously increased by decreasing exhaust pressure. As respective flame-holding elements were visually observed to blow-out, data points were recorded at the conditions of each blow-out. Because any one air flow gave specific combinations of inlet pressure and velocity, several air flows were run to permit possible segregation of the pressures and velocity effects. The procedure was then repeated at other values of fuel-air ratio.

CONCEPTS OF FLAME-HOLDER DESIGN

As mentioned in the INTRODUCTION, 7 different design concepts were embodied in the 31 flame-holder elements studied. These will be classed as types 1 through 7. The design concepts of each type will be discussed briefly and the variations within each type will be shown in sketches given in figures 5 through 11. Front and rear quarter photographs of the three test assemblies used are shown in figure 2. The elements tested with each assembly are listed in table I.

Type 1. - Type 1 (fig. 5) included 6 elements, 1A to 1F, and consisted of variations of the basic V-gutter flame holder. Elements 1A and 1D actually were identical except for tip plates which were installed in 1D. These elements were used as standards of comparison on the three assemblies used. Flame-holder element 1B was different from 1A only in the matter of metal thickness; it was reasoned that the inside surface temperatures of element 1B with a metal thickness of 0.125 inch might be higher than element 1A with thickness of 0.0625 inch and hence improve the stability limit. Element 1C was run to determine the effect of an uncooled splitter plate on stability. Such splitter plates (water-cooled) tend to suppress screech in afterburners (ref. 4). An increase in gutter width from 1 to $1\frac{3}{8}$ inches was made in element 1E, while an increase in gutter width to $1\frac{7}{8}$ inches was made in element 1F to determine the effect of gutter width on the stability of type 1 elements. Tip plates were incorporated in all elements used in assembly 3, 1D, 1E, and 1F, to eliminate any possible effect of the assembly support struts on the comparison between the elements of this assembly.

Type 2. - This type comprised 6 elements, 2A to 2F. A typical element is shown by the sketch of figure 6(a). It may be supposed that if

flame-holder elements were submerged in the flame from another element upstream, the stability and perhaps efficiency would be improved because of the higher approach temperature of the gas to the latter elements and because of their higher surface temperatures. A cross section of the type 2 configurations shown in other parts of figure 6 may be regarded in this light, each depression representing a successive flame seat area. In addition, the direction of the corrugations was chosen at an angle to the direction of the gas flow in an attempt to produce an outflow near the surface of the element. Such an outflow was desired in order to provide ignition sources beyond the radial span of the element, and also to promote mixing due to secondary flows in the combustion chamber downstream of the flame-holder element. The desired secondary flow patterns are shown in the following sketches:

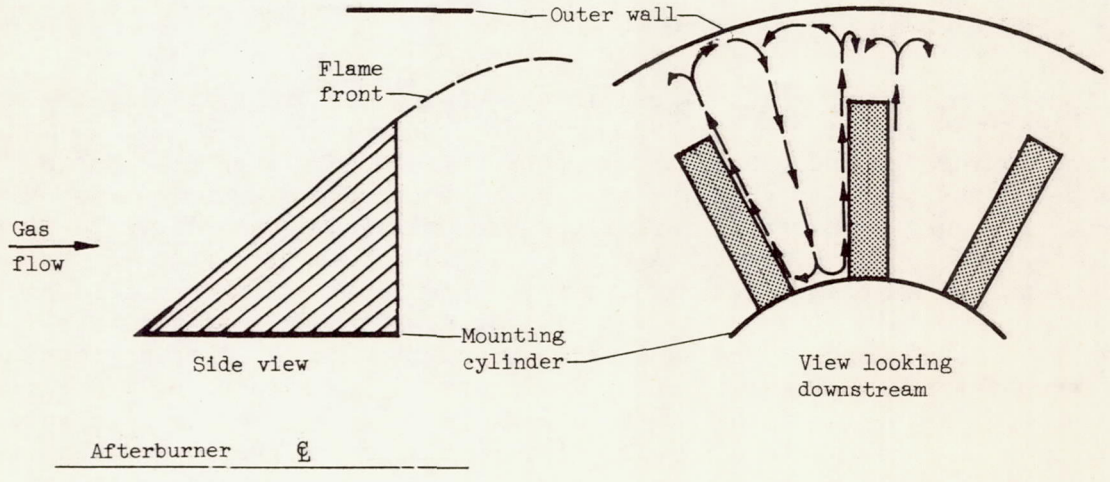

Type 3. - This type, shown in figure 7, is similar to the type 2 family except that it was intended to produce a stronger radial flow by introducing gas flow into the depressions formed by the vanes near the leading edge. It was recognized that this through-flow in the recirculation region might reduce the stability limits; possible improvements in propagation and mixing, however, warranted its inclusion.

Type 4. - The principle upon which this type, illustrated in figure 8(a), is based is simply the use of screens (or other types of blockage) to reduce the local velocity in which an otherwise conventional element may operate. In the representative elements used herein, 4A to 4L, the screens are graded in 2 or 3 steps to produce a gradual velocity gradient at the trailing edge, in keeping with reference 5 where it was found that flame did not propagate well across a steep gradient. The anticipated flow pattern around a typical element is shown in the following sketch:

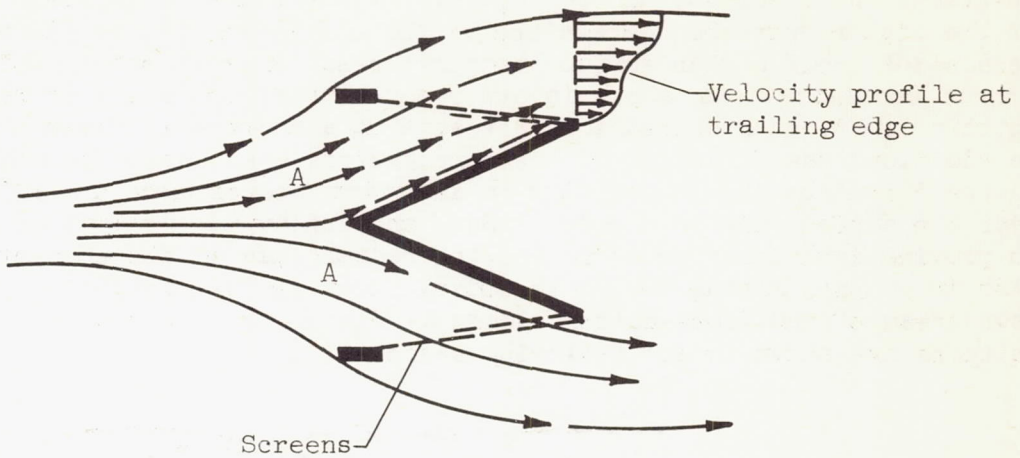

Diffusion of the approach stream is expected to occur in the regions marked A because of the damming effect of the screens, and as a result the velocity through and behind the screens is reduced. The anticipated shape of the velocity gradient is also shown in the sketch. As is evident in figure 8, numerous variations were studied in an effort to optimize this type. Elements 4A through 4G were relatively simple variations on the simple V-gutter; however, elements 4H and 4I are more complex. Element 4H (fig. 8(i)) was similar to 2D shown in figure 6(e), except that screens of graded density were added to the leading edges of the element. Element 4I shown in figure 8(j) was identical to element 4A except for the addition of the end plate and the 6 small cross gutters. These small cross gutters were of different size and shape, and were intended to explore the possibilities of obtaining adequate stability limits for these very small elements by virtue of the supporting action (with regard to combustion) provided by the large element to which they were attached.

Type 5. - Two elements, 5A and 5B, figure 9, were attempts to construct flame-holder elements along the line of small can-type combustors. The general configuration is shown in figure 9(a). Because of the indication that wall quenching effects prevent the extrapolation of combustor design rules in the literature to so small a scale, no attempt was made to apply the rules regarding hole-area distribution in the design of 5A. In accordance with unpublished work on can-type combustors, however, the pilot area was chosen to be about 60 percent of the channel flow area, proper slope of the walls was maintained, no fuel was introduced closer to the upstream end of the pilot than one pilot diameter, and the ratio of hole area to capture area was selected as 0.69.

Element 5B was designed to provide a static pressure ratio of 1.1 across the holes in the liner by consideration of flame-holder blockage in the duct (which sets the static pressure inside the liner) and by setting the diffusion rate between the liner and shroud (which determines static pressure upstream of the holes). This value of 1.1 has been found experimentally to give good stability limits at low pressure levels.

Type 6. - This type of flame holder is represented only by 1 element, 6A (fig. 10). The concept employed is the use of either air or fuel injection in such a manner as to increase the recirculation of hot gasses in the wake of the gutter element. For this particular design, the injected fuel or air (each was tried separately) is designed to produce an ejector action between the two parallel plates, figure 10(a), and thus, by entrainment of hot gasses, increase the recirculation. Such a method was employed elsewhere (unpublished) in a pilot-type configuration, and a blow-out velocity of over 1000 feet per second was achieved.

Type 7. - Several years ago at the Lewis laboratory it was found that it is possible to stabilize flame in a stagnation region on the upstream edge of a flame-holder element. This principle was employed in the design of elements 7A to D (fig. 11). In element 7A, this principle was used in conjunction with another concept, that of using one large element to support many small elements which would in themselves have very poor stability limits. As shown by the arrows in figure 11(a), the flow would be virtually stagnated in the leading edge depression of the main element marked A, where combustion would occur. The high pressure would then force a gradual flow of hot gasses outward within the smaller cross gutters. Finally these gasses would be discharged gradually from the cross gutters, thereby providing ignition sources to support combustion on the cross gutters. It is considered important that the rearward discharge jets from the cross gutters be along the inner surfaces of the cross gutter rather than on the gutter centerline so the tendency is to augment rather than oppose the normal recirculatory flow produced by the cross gutter.

The stagnation concept was also used in combination with screen for elements 7B and 7C (figs. 11(c) and (d)) to gain possible advantages from both principles.

Element 7D shown in figure 11(e) was designed to provide a more quiescent stagnation region A by the use of a double-walled construction. A portion of the gas flow enters the stagnation region A (where combustion occurs) through three slots in the leading edge. The hot gasses of combustion pass from the stagnation region rearward between the parallel walls and discharge in a rearward direction at the edges of the gutter, thus tending to reinforce the normal recirculation with additional ignition sources.

RESULTS AND DISCUSSION

In interpreting the results of this study it is important that the values of blow-out velocity reported herein be considered in the proper light. Because of the higher blockage of an element when it is supporting combustion than when it is not, the damming action of the elements changes and causes local velocities to change as the various elements blow out. Thus for a given bulk velocity (local velocities were not measured), the local velocity would be higher for an element operating in a group of good elements, which are burning, than it would for the same element in an assembly of poor elements, most of which are out. The bulk velocity values presented herein indicate only the relative order of merit of the elements in a given test assembly rather than qualitative limits. Thus comparisons between various test assemblies are not valid.

Assembly number 1. - The stability limits of the elements of assembly number 1 (fig. 2(a) and (b)) were first determined at an average fuel-air ratio of 0.0405 and are presented in figure 12(a). The solid symbols denote element 1B, the 1-inch V-gutter that was used as a reference for determining the relative performance of elements in this assembly. Except for the screen-type element, most elements blew out before the standard V-gutter did. In these runs, element 4A, the screen-type gutter, had outstanding performance with blow-out occurring at bulk velocities much higher than the other elements. Other runs of assembly number 1 in which element 3A, radial vanes, was replaced by element 4B, V-gutter with screens, are shown in figures 12(b), (c), and (d) at fuel-air ratios of 0.038, 0.045, and 0.0515, respectively. In one instance, a large number of elements blew out simultaneously and thus a cluster of symbols about a certain point occurs. In these figures, element 1B, the V-gutter, is again used as the reference element.

For an afterburner having a bulk velocity of 600 feet per second (as discussed in the INTRODUCTION), the peak local velocity at a given element might well be on the order of 750 feet per second. Hence, in the consideration of data such as those shown in figure 12, any element blowing out at velocities below 750 feet per second would appear unsuitable for use in a high-velocity afterburner from a stability standpoint.

To simplify comparisons, the performance of the different elements of assembly 1 is given in the form of bar charts in figures 13, 14, and 15. The relative performance of the 3 standard-V elements is shown for several fuel-air ratios in the bar charts of figure 13. The blow-out velocity of each element is presented as a percentage of the blow-out velocity of the standard-V element 1B. In all cases several runs were averaged to eliminate possible random or erratic effects.

The effect of metal thickness may be seen by comparing elements 1A and 1B. At fuel-air ratios of 0.04 and above, the V-gutter with 0.125-

inch metal was superior to the V-gutter with 0.063-inch metal thickness. The V-gutter with a splitter plate extending 7 inches downstream of the trailing edge likewise showed promise only at the highest fuel-air ratio tested, indicating a possible benefit of flame-immersed metal and hotter surfaces for rich fuel-air operation.

The relative blow-out velocities of the type 2 elements, the slant type, are compared in figure 14. With very few exceptions the majority of these elements blew out before the standard-V element. At a fuel-air ratio of 0.038, blow-out velocities were between 66 and 91 percent of the reference blow-out velocity. Above that fuel-air ratio the elements with from 2 to 4 ripples of corrugations (2A, 2B, 2C) blew out at widely scattered velocities. The element with 4 ripples (2C) proved much less stable than the element with 3 ripples (2A), while the element with 2 ripples (2B) gave intermediate performance. The elements with sharp flame-seating edges (2E, 2F) were definitely better than the other type 2 designs at the higher fuel-air ratios. At a fuel-air ratio of 0.045 the blow-out limit of the saw-tooth corrugation element (2E) was 125 percent of the blow-out limit of the reference element in the assembly, while the staggered-slanted V-gutters of element 2F showed the biggest improvement of stability as fuel-air ratio increased. Despite the generally unsatisfactory performance of group 2 elements over a broad fuel-air range, they did accomplish their design objective by spreading flame from 1 to $1\frac{1}{2}$ inches beyond the tip of the element.

Although not shown, at a fuel-air ratio of 0.0405 the radial-flow-type element 3A had a blow-out velocity of only 60 percent of the standard-V element. This was the only fuel-air ratio at which element 3A was tested and, because of its initial poor performance it was discarded as unsatisfactory. A comparison of the other elements tested in the first assembly is shown in figure 15. At a fuel-air ratio of 0.038, the screen-type elements had a blow-out velocity 40 percent higher than that of the standard-V element.

Operation of assembly 1 at higher fuel-air ratios indicated a drop in advantage of the screen-type elements, but even at a fuel-air ratio of 0.0515, their performance was better than that of the standard-V element. The higher density of screening in element 4B resulted in somewhat poorer performance than the initial screen element 4A, the differences being very slight. Over the fuel-air range tested the can-type element 5A had a blow-out velocity between 84 and 96 percent of the reference blow-out velocity, with operation at the lean region more favorable.

Assembly number 2. - The performance curves for the second test assembly (fig. 2(c) and (d)) are presented in figure 16 for values of fuel-air ratio between 0.024 and 0.065. A solid symbol again identifies the reference standard-V element, 1A in this assembly. The conventional V-gutter (1A) was among the best elements for all conditions investigated.

The comparative performance is again discussed with the aid of bar charts of figures 17 to 20. After the completion of testing with assembly 2, damage was noted in several of the screen-type elements. Local areas were found where screens had parted slightly from the trailing edge of the gutter; hence, in such cases the advantages of the screen principle may have been practically lost. In regard to scale (gutter width), the relative performance of type 4 elements with 1/2-, 3/4-, and 1-inch gutters is shown with bar graphs at several fuel-air ratios in figure 17. At a fuel-air ratio of 0.024, the 1-inch gutter was the best while the 1/2-inch gutter was the worst in stability, the latter having a blow-out velocity 40 percent of the former (fig. 17(a)). At a fuel-air ratio of 0.0625 the order of blow-out was reversed, with the 1/2-inch gutter blowing out at a velocity 79 percent of the standard-V (fig. 17(d)). Because the 1-inch element 4(d) had high screen density (meshes of number 10, 16, and 28 screens in varying amounts) while the other screening incorporated only meshes of number 10 and 16, these results on the effect of scale are considered only as being indicative of the trend. The progressive improvement of the 1/2-inch element 4E and deterioration of the 3/4-inch and 1-inch elements at increased fuel-air ratio are not understood. Behavior of this type might indicate an inertia-separation-effect on fuel droplets, although a long (31-inch) mixing length was used.

The effect of upstream-screen capture dimension of the screens may be seen by comparing elements 4C and 4D in figure 18. Above a fuel-air ratio of 0.0505, the 1-inch screen was the most stable of all elements in the assembly. At a fuel-air ratio of 0.024 the $1\frac{1}{2}$-inch screen proved the most stable, with the blow-out velocity of the 1-inch screen 33 percent less. The effect of the screen location is also shown in figure 18 by comparing element 4D with element 4F. Above a fuel-air ratio of 0.0375 the blow-out velocity of the downstream-screen element (4F) was 12 to 15 percent higher than the blow-out velocity of the upstream-screen element (4D). At the fuel-air ratio of 0.024, the $1\frac{1}{2}$-inch upstream-screen element was by far superior to the downstream-screen element. The data of both figures 17 and 18 indicate the sensitivity that the screen-type elements have to fuel-air ratio and that no element tested operates as well as the standard-V-gutter over a broad range of fuel-air ratios. Although use of screens aids stability, the optimum capture dimension, scale, and density of the screening can be markedly affected by fuel-air ratio and no easy design rules can be formulated.

The relative performance of several other types of elements of the second assembly is shown in figure 19. As fuel-air ratio increased from 0.024 to 0.0625, blow-out velocities of the slant-type element augmented with upstream screens (4H) increased from 62 to 84 percent of the reference velocity. This performance was poorer than the original slant element without the screen. The peak performance of the can-type element

5B was reached at a fuel-air ratio of 0.0375 where blow-out occurred at a velocity of about 80 percent of that for the standard-V. At other fuel-air ratios, its performance was quite poor. Employment of the ejector principle in element 6A gave performance intermediate between that of the can-type element 5B and the standard-V element, with operation at lean fuel-air ratio most favored.

The performance of several type 7 elements, stagnation type, which were also tested in assembly number 2 is presented in figure 20. The stagnation concept which this type employs showed little promise above a fuel-air ratio of 0.0375. Below this fuel-air ratio their performance was only slightly poorer than the standard-V gutter. Performance deteriorated rapidly with an increase in fuel-air ratio so that at a fuel-air ratio of 0.0625, the blow-out velocity of element 7C was 35 percent of the reference, while the blow-out velocity of element 7A was about 70 percent of the reference. In connection with element 7A, it was noted that its smaller side gutters derived considerable support for combustion from the larger main gutter in that both elements blew out together despite the large difference in gutter width.

Assembly number 3. - Assembly number 3 (fig. 2(e) and (f)) comprised elements of only 3 types - the standard-V, the screen-type, and the stagnation type. Each element incorporated an end plate that extended 1/4 inch beyond the leading edges of a V-gutter and 1 inch downstream of the trailing edge. For the sake of clarity these end plates, although seen in the photograph of the assembly in figure 2(e) and (f), were not shown on the diagrams of figure 8 for elements of type 4.

The stability limits of the elements in assembly number 3 are presented in figure 21 at several fuel-air ratios. Element 1D, the 1-inch-wide V-gutter, was used as the standard reference as it was similar to element 1A of assembly number 2 except for the tip plate. At two of the runs at an average fuel-air ratio of 0.0405, several elements remained lit when the facility limited the maximum velocity and the minimum total pressure obtainable. Erratic behavior, encountered in several runs, produced blow-out of a number of elements simultaneously as well as unusually premature blow-out of the 1-inch standard V-gutter. These data are consequently not reliable. Generally speaking, the standard-V-gutter of $1\frac{7}{8}$-inch width was by far the most stable of all elements tested in this assembly.

The relative performance of the elements of this assembly is given by bar charts in figure 22 for an average fuel-air ratio of 0.0405. A marked improvement in blow-out velocity occurred when the width of the standard V-gutter was increased from 1 to $1\frac{3}{8}$ inches. The gutter with a width of $1\frac{7}{8}$ inches was similar in performance to the $1\frac{3}{8}$-inch gutter,

although in several instances this element remained lit at the completion of a run. This improvement in performance with gutter width agrees with other studies (refs. 6 and 7).

As shown in figure 8, several small gutter elements were attached to the main gutter to determine whether the main gutter would support the smaller ones, thus allowing their use to spread the flame. Observations showed that as the velocity was increased, the small gutters ceased progressively from the tip to hold flame until about one half of the span was out. At this condition, the main gutter failed to support combustion. Thus about one-half of the length of the small cross gutters remained lit as long as the main element held flame, indicating that support was derived from the main gutter and also that such small gutters may be useful in producing a rapid spread of the flame front.

CONCLUDING REMARKS

From this brief exploratory study of flame-holder shapes intended for use at high afterburner velocities, it was found that a screen-type flame holder could far exceed the velocity limits of the same size conventional V-gutter at fuel-air ratios below about 0.045. The screen-type flame holders were, however, sensitive to fuel-air ratio. In contrast, the conventional V-gutter was not sensitive to fuel-air ratio and had better stability limits than any other type except in the range for fuel-air ratios below 0.045 where a particular screen-type was optimum. It was found that increased metal temperature (thicker metal or splitter plates) may be beneficial at high fuel-air ratios. The use of small finger-like gutters to spread the flame from a large main gutter appeared promising inasmuch as the stability limits of the small gutters were increased (over most of their length) to that of the main gutter by the piloting action of the main gutter.

Lewis Flight Propulsion Laboratory
National Advisory Committee for Aeronautics
Cleveland, Ohio, October 7, 1954

REFERENCES

1. Gabriel, David S., Krebs, Richard P., Wilcox, E. Clinton, and Koutz, Stanley L.: Analysis of the Turbojet Engine for Propulsion of Supersonic Fighter Airplanes. NACA RM E52F17, 1953.

2. Zettle, Eugene V., Norgren, Carl T., and Mark, Herman: Combustion Performance of Two Experimental Turbojet Annular Combustors at Conditions Simulating High-Altitude Supersonic Flight. NACA RM E54A15, 1954.

3. Nakanishi, S., Velie, W. W., and Bryant, L.: An Investigation of Effects of Flame-Holder Gutter Shape on Afterburner Performance. NACA RM E53J14, 1954.

4. Usow, Karl H., Meyer, Carl L., and Schulze, Frederick W.: Experimental Investigation of Screeching Combustion in Full-Scale Afterburner. NACA RM E53I01, 1953.

5. Anon.: Survey of Bumblebee Activities. Bumblebee Series Rep. No. 121, Appl. Phys. Lab., Johns Hopkins Univ., Feb. 1950. (Contract NOrd 7386 with Bur. Ord., U.S. Navy.)

6. Henzel, James G., Jr., and Bryant, Lively: Investigation of Effect of Number and Width of Annular Flame-Holder Gutters on Afterburner Performance. NACA RM E54C30, 1954.

7. Renas, Paul E., and Jansen, Emmert T.: Effect of Flame-Holder Design on Altitude Performance of Louvered-Liner Afterburner. NACA RM E53H15, 1953.

TABLE I

ELEMENTS TESTED WITH EACH ASSEMBLY			
Group	Assembly		
	No. 1	No. 2	No. 3
1	A, B, C	A	D, E, F
2	A, B, C, D, E, F	-------	-------
3	A	-------	-------
4	A, B	C, D, E, F, G, H	D, F, I, J, K, L
5	A	B	-------
6	-------	A	-------
7	-------	A, B, C	A, D

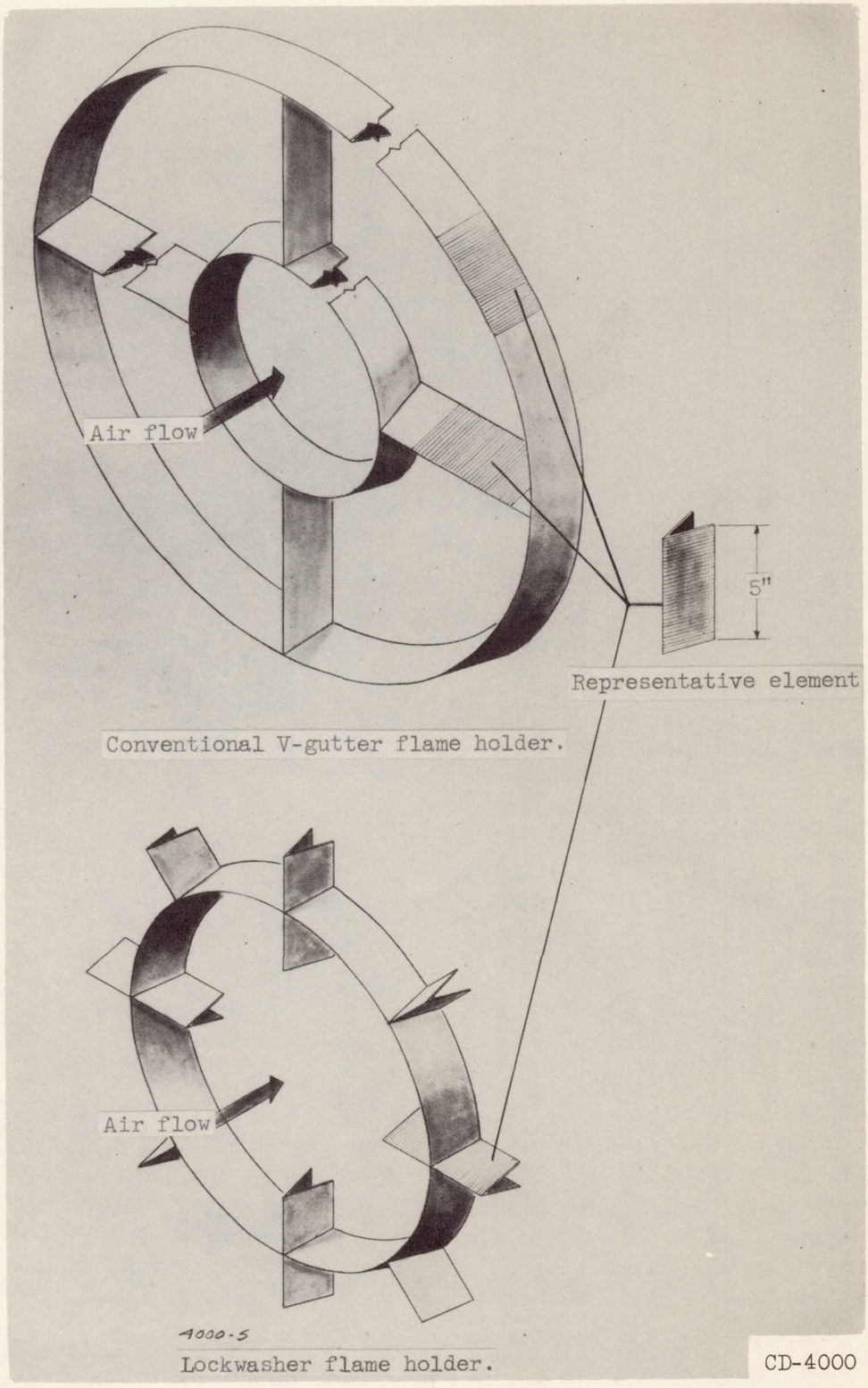

Figure 1. - Relation between representative element and complete flame holder.

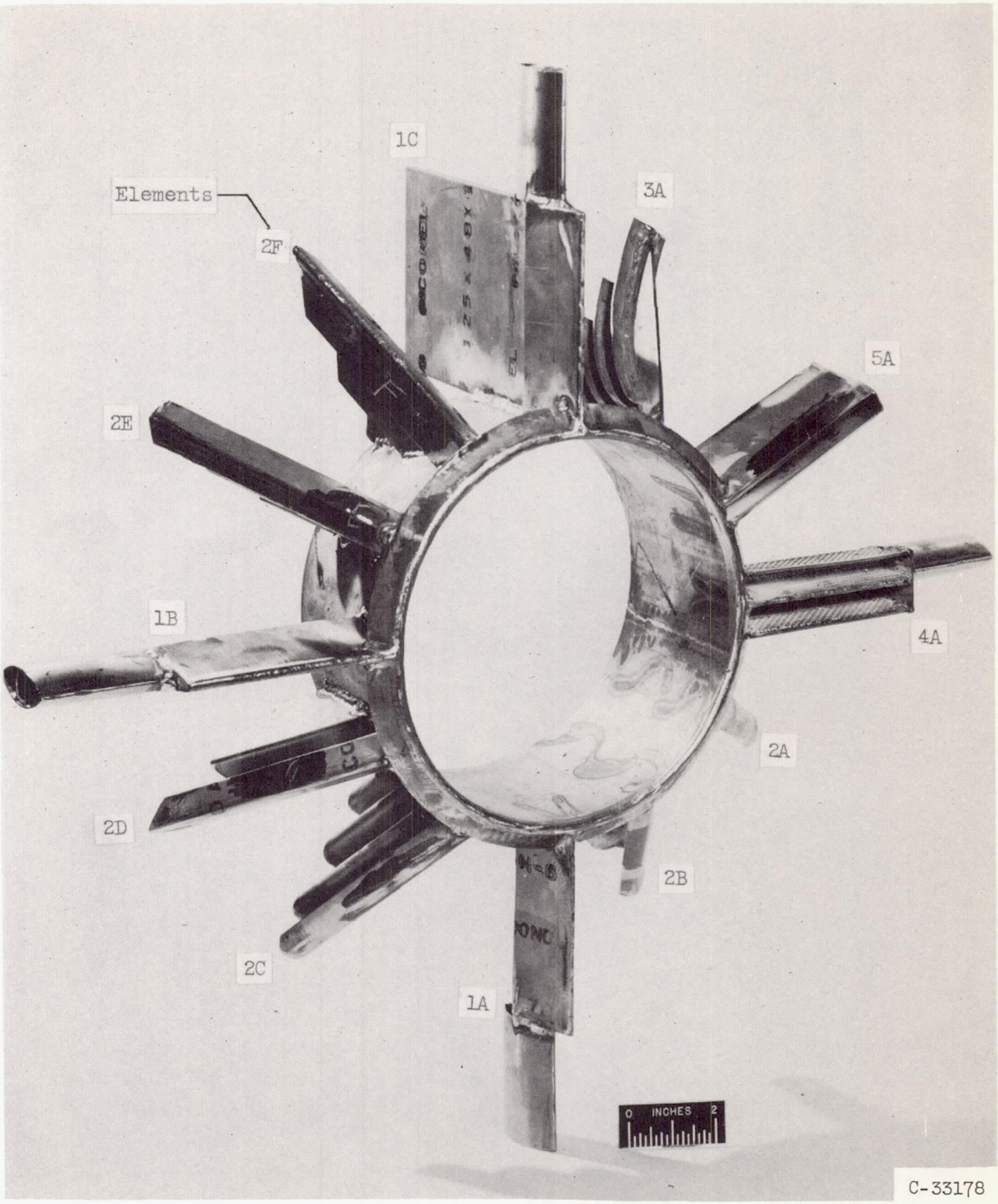

(a) Front quater view of assembly 1.

Figure 2. - Test assemblies.

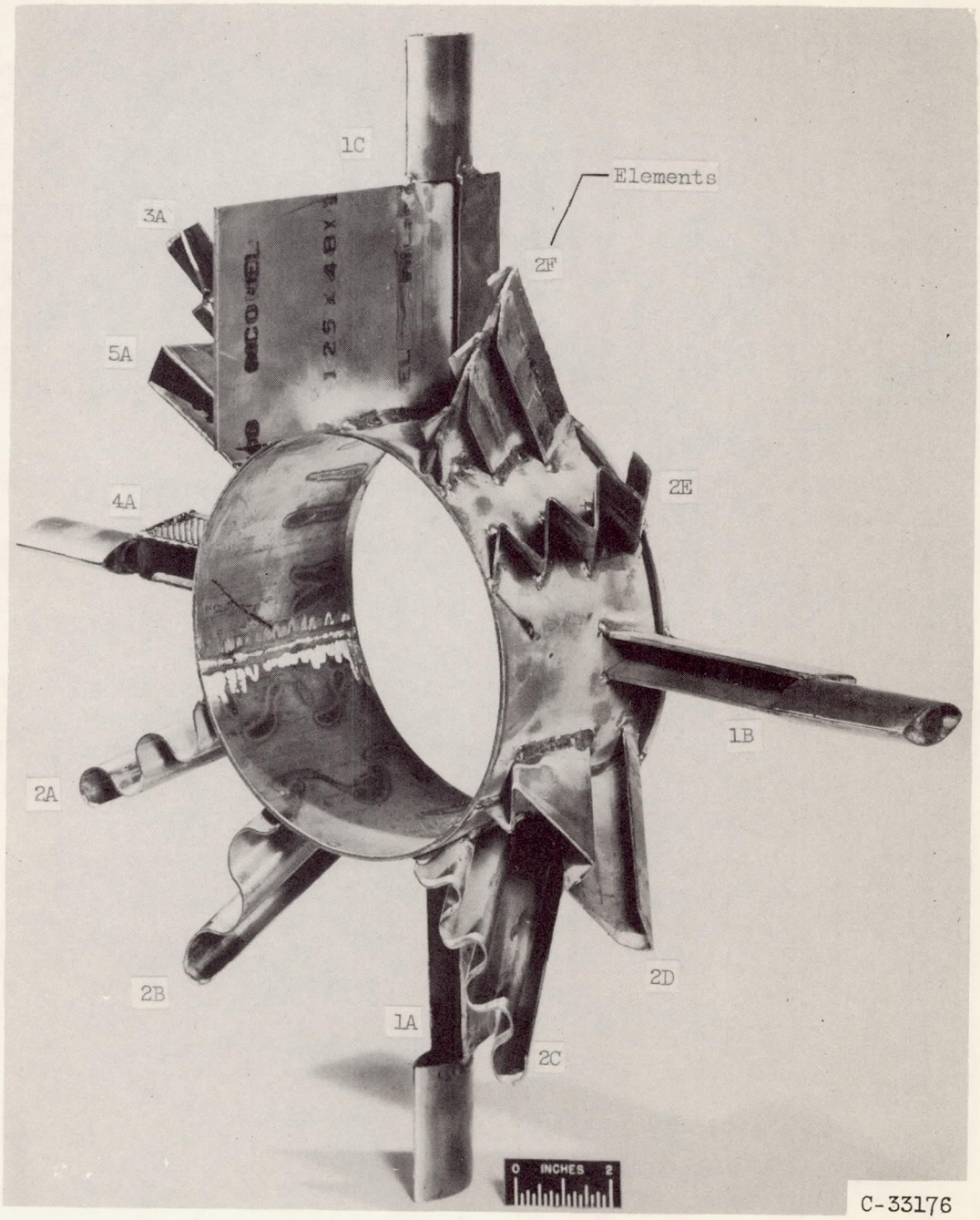

(b) Rear quarter view of assembly 1.

Figure 2. - Continued. Test assemblies.

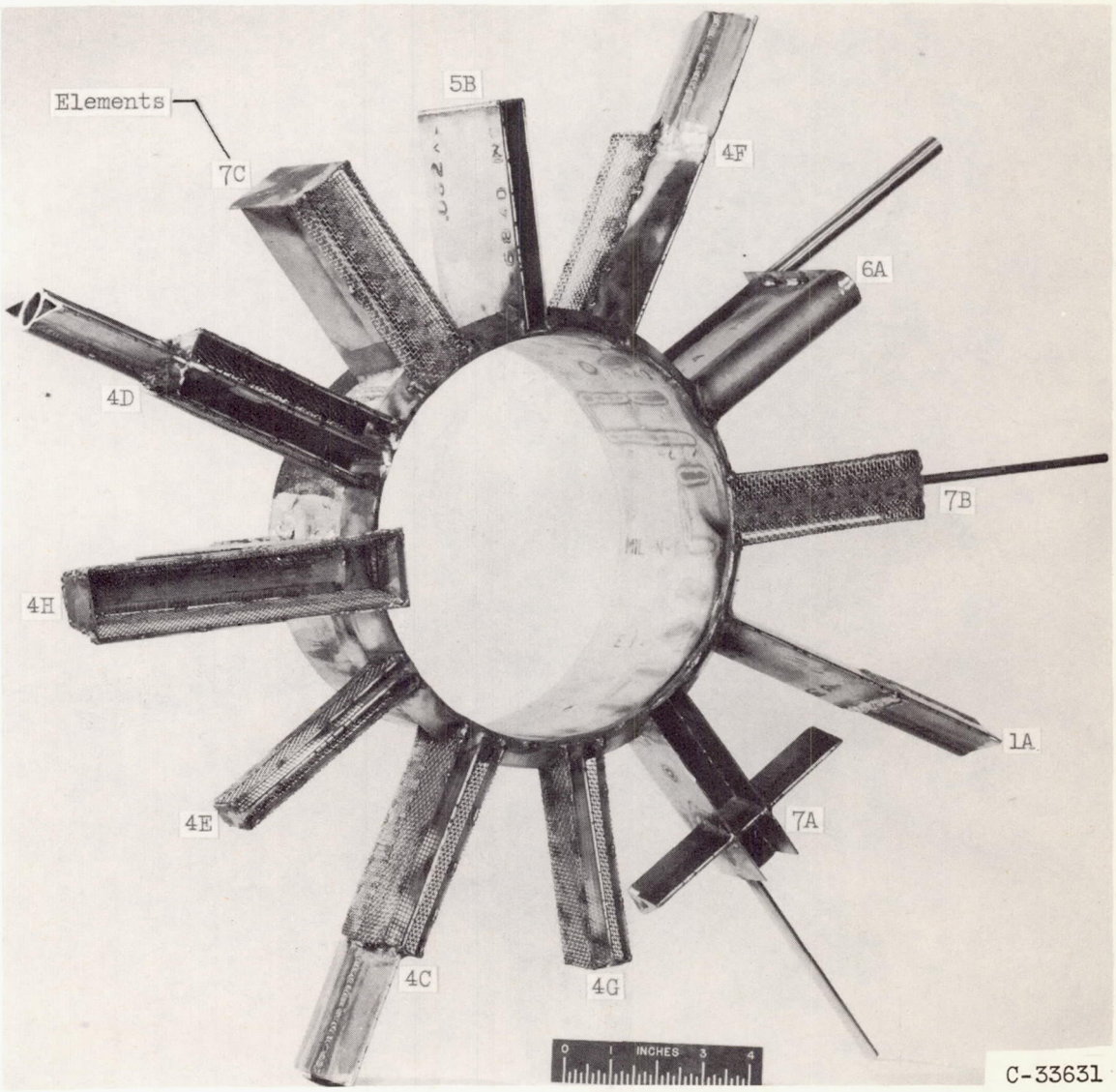

(c) Front quarter view of assembly 2.

Figure 2. - Continued. Test assemblies.

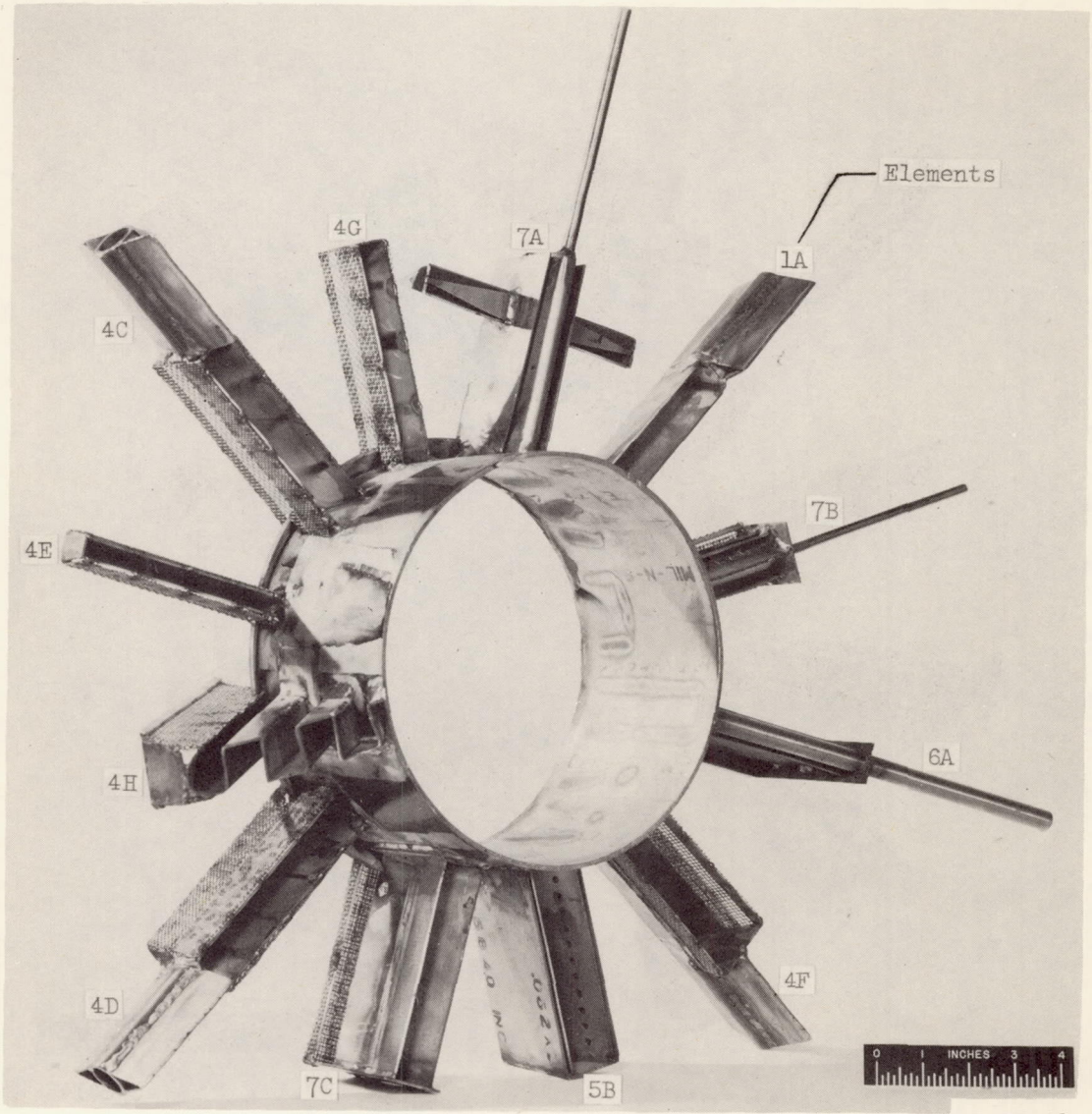

(d) Rear quarter view of assembly 2.

Figure 2. - Continued. Test assemblies.

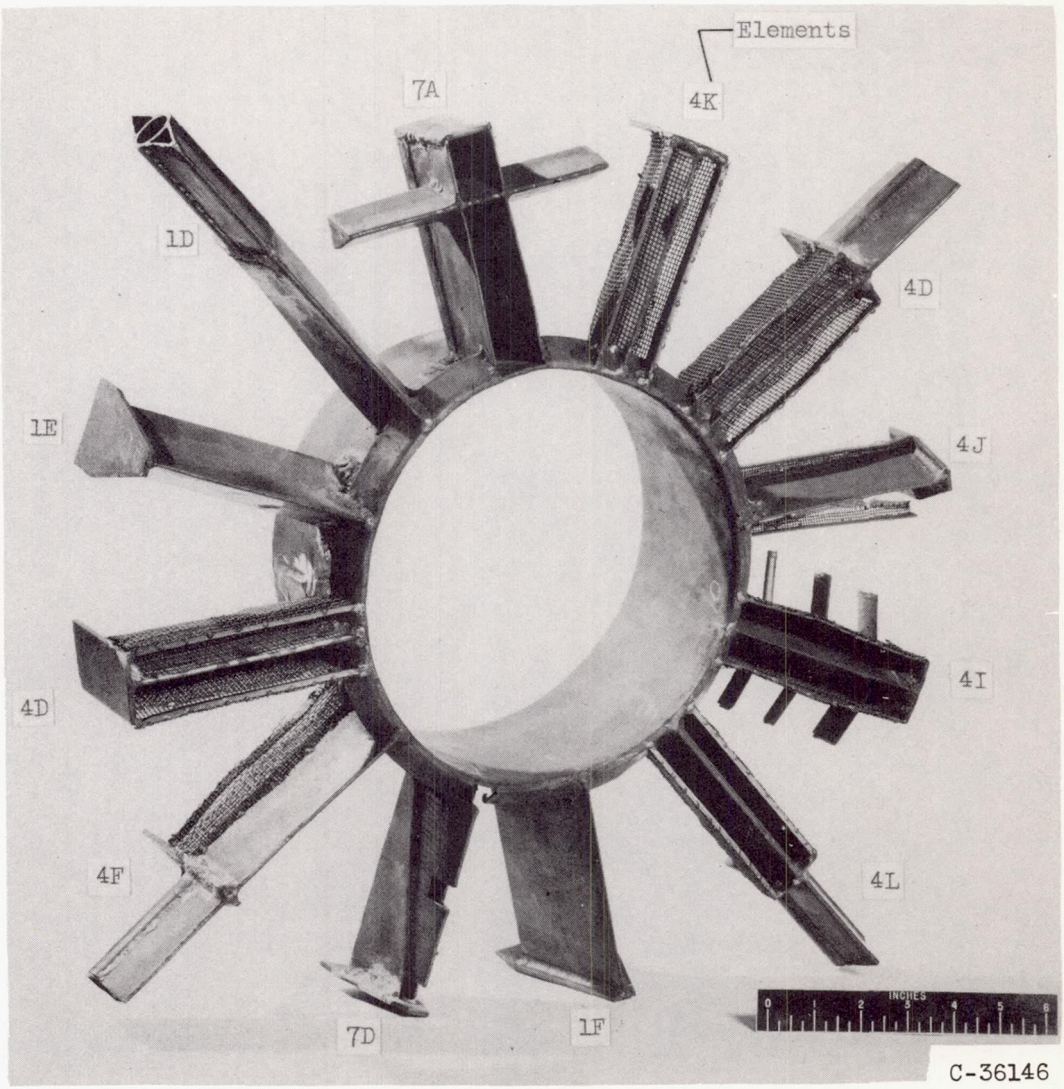

(e) Front quarter view of assembly 3.

Figure 2. - Continued. Test assemblies.

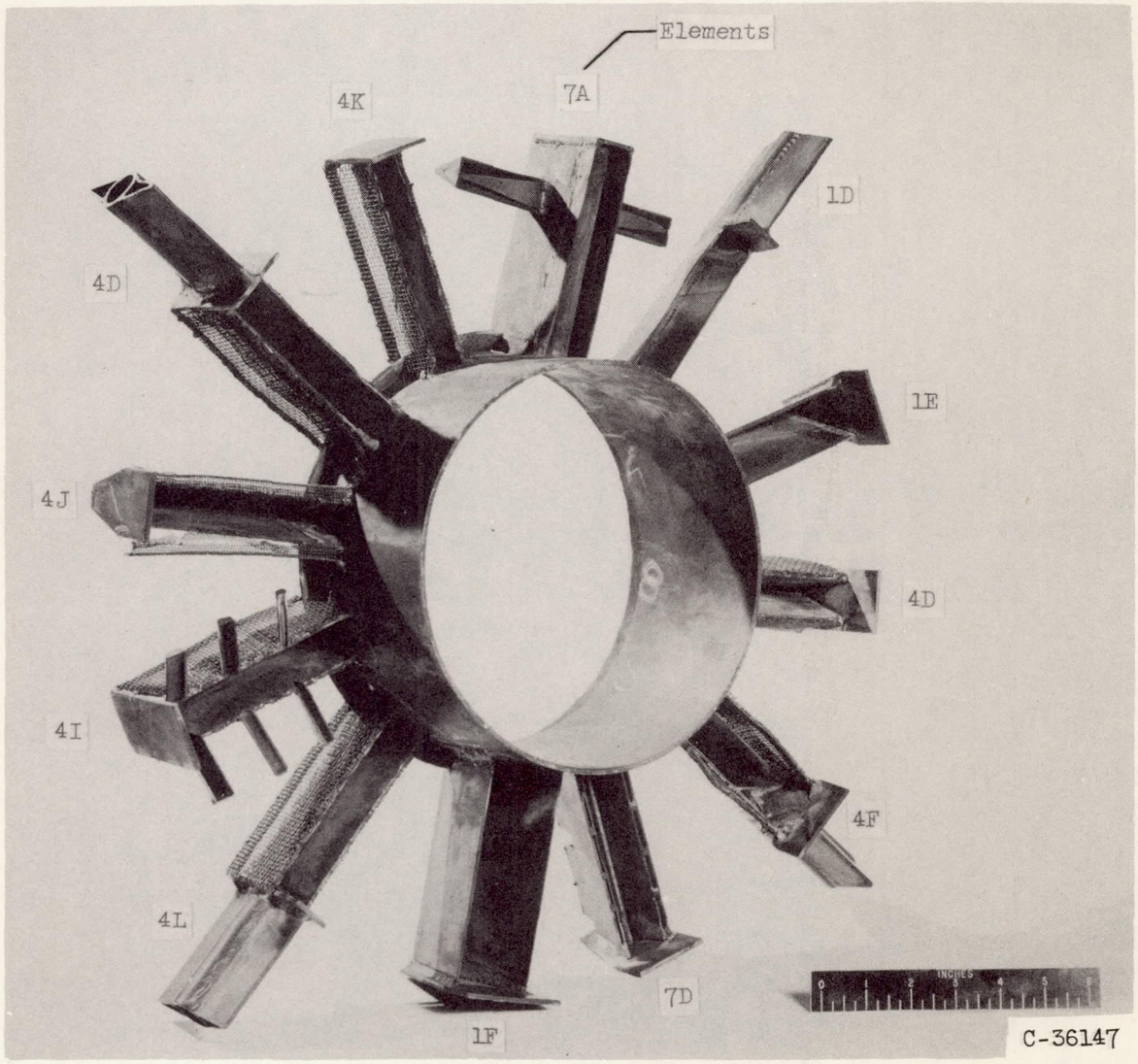

(f) Rear quarter view of assembly 3.

Figure 2. - Concluded. Test assemblies.

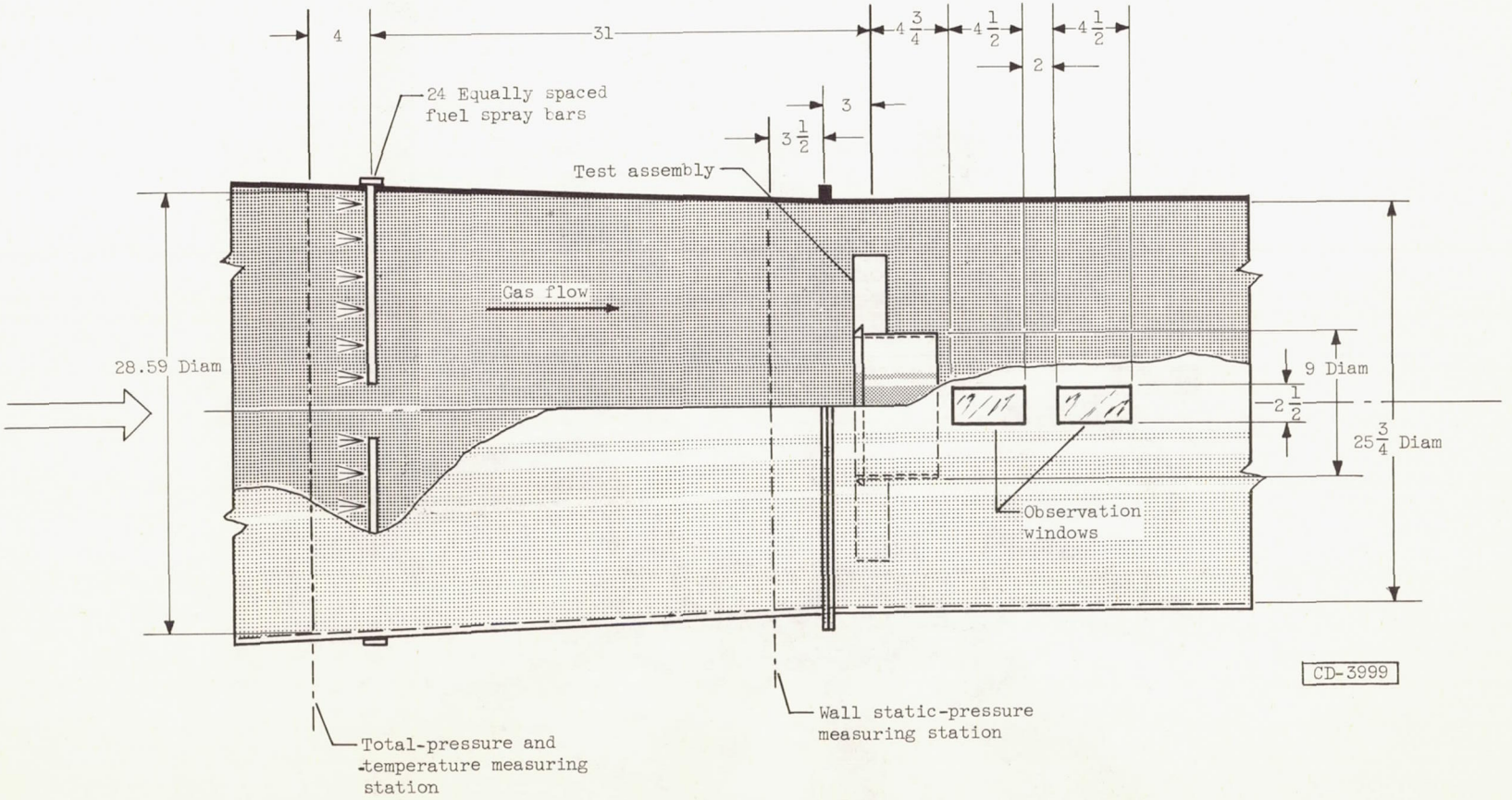

Figure 3. - Sketch of test section. (All dimensions in inches.)

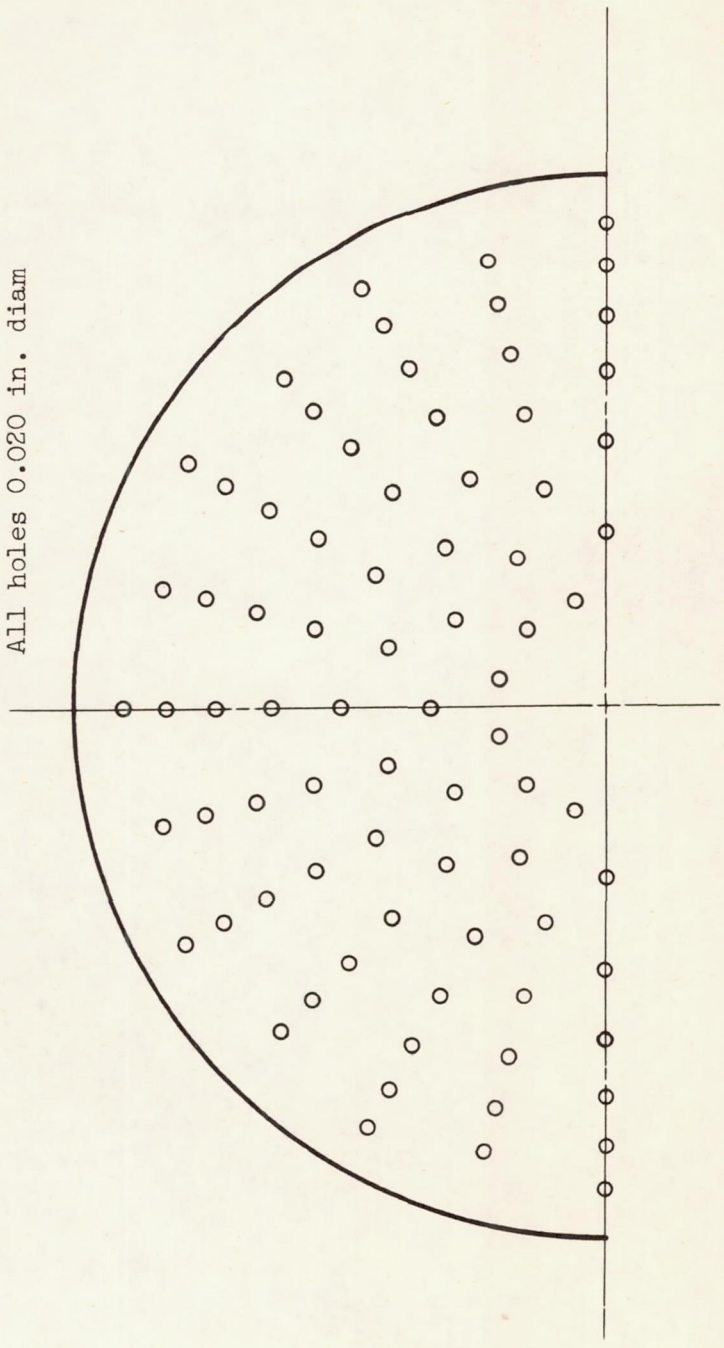

Figure 4. - Fuel distribution pattern.

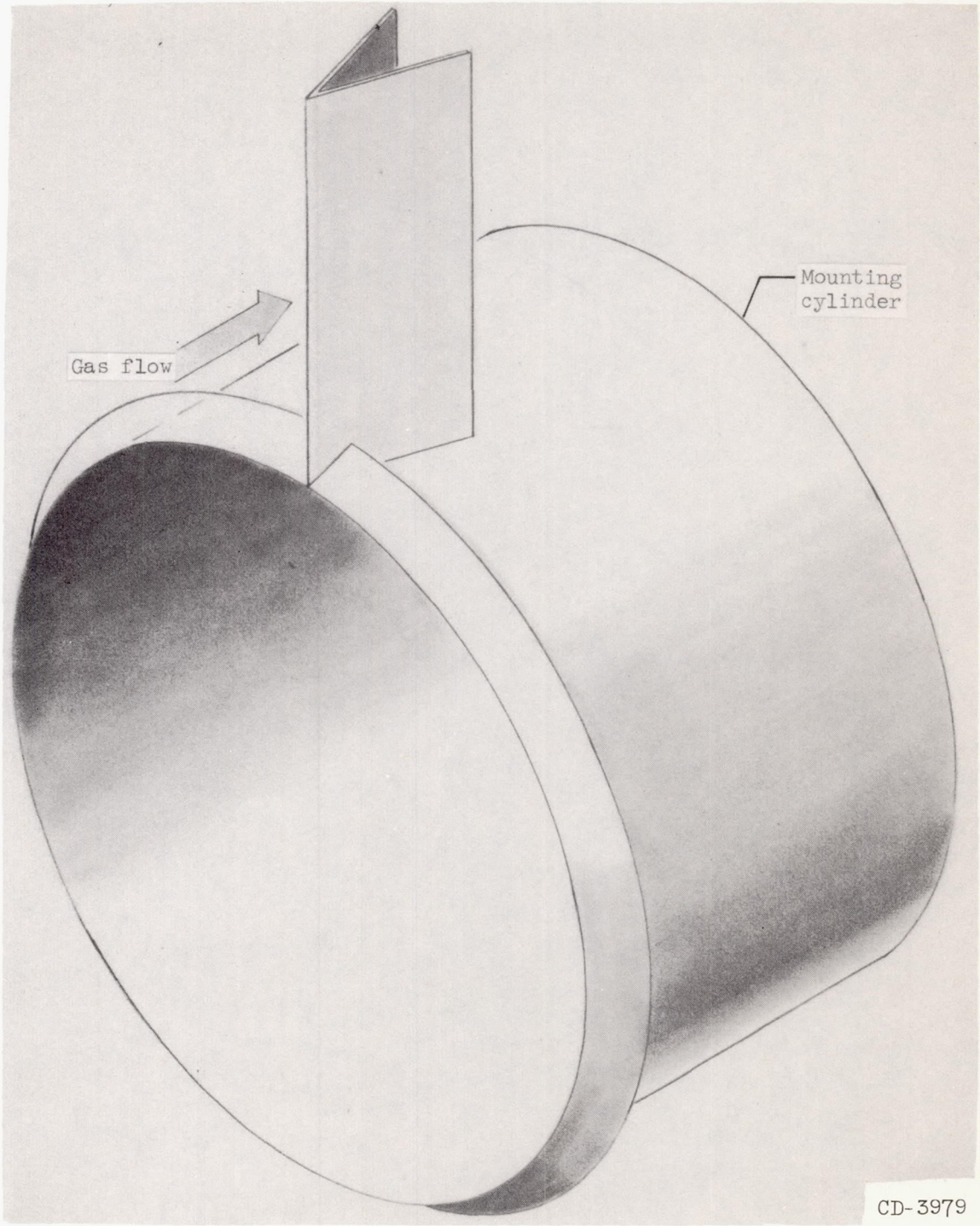

(a) Typical type 1 flame holder element.

Figure 5. - Sketches of type 1 flame holding elements investigated.
(All dimensions in inches.)

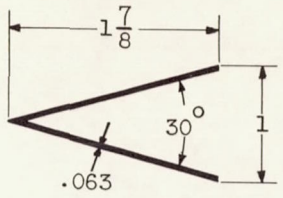

(b) Element 1A.

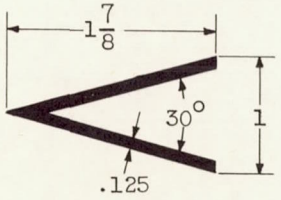

(c) Element 1B.

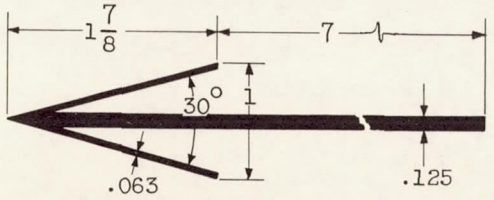

(d) Element 1C.

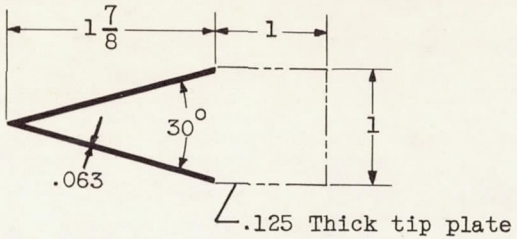

(e) Element 1D.

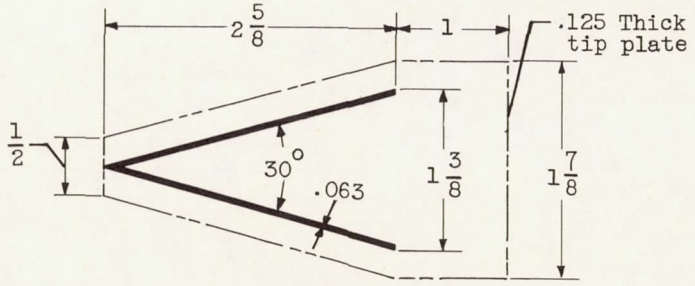

(f) Element 1E.

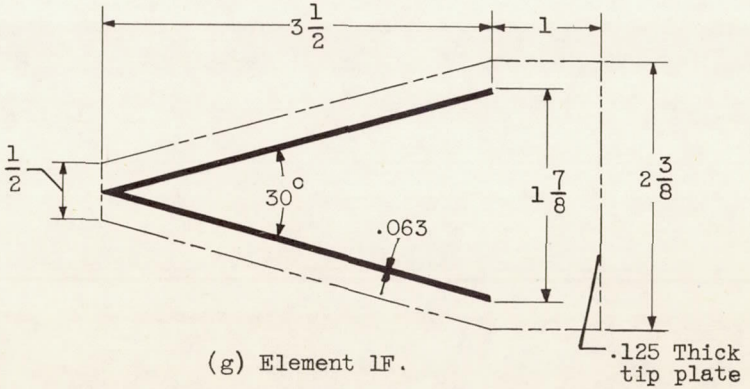

(g) Element 1F.

CD-3987

Figure 5. - Concluded. Sketches of type 1 flame holding elements investigated. (All dimensions in inches.)

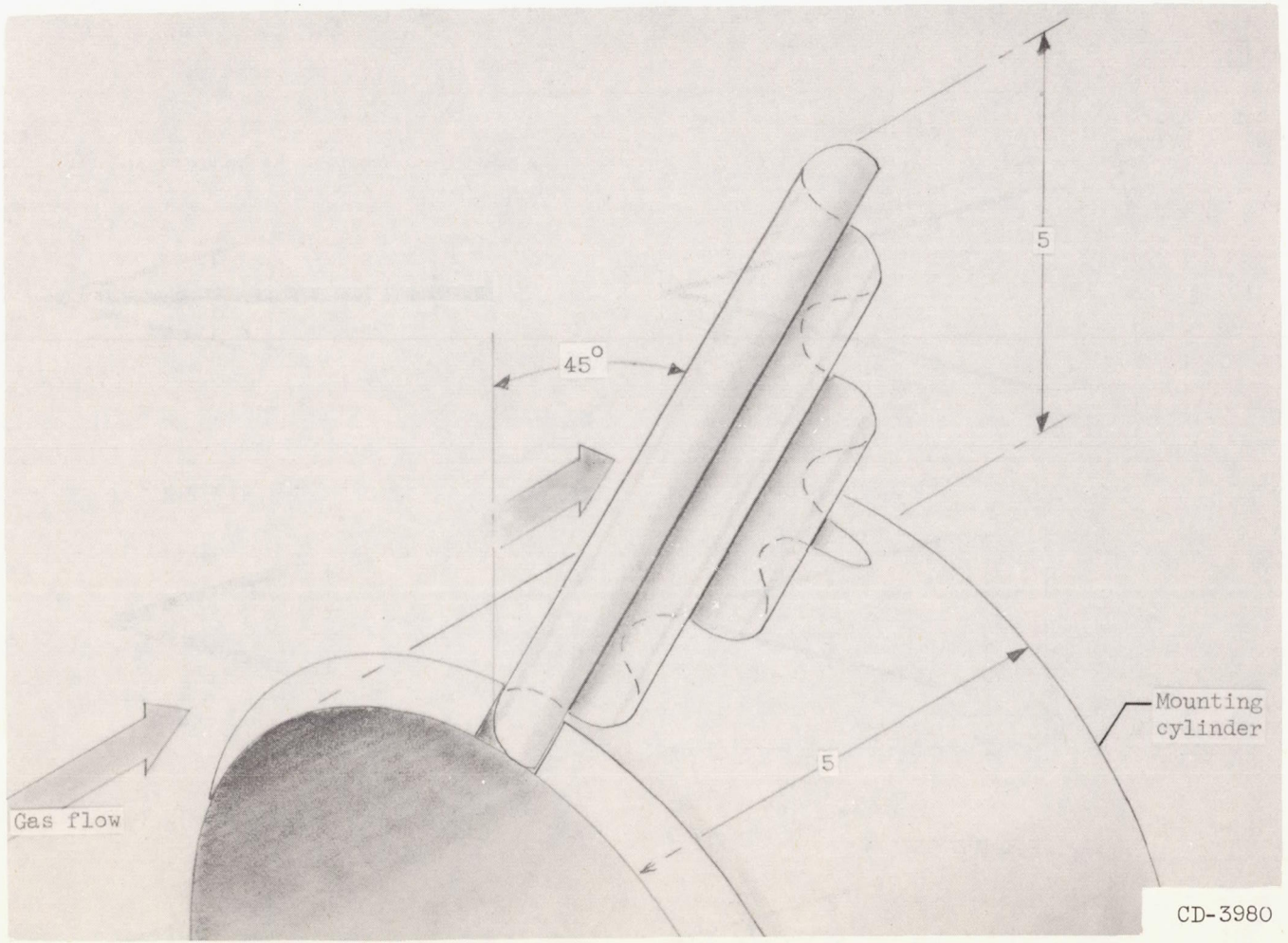

(a) Typical type 2 flame holder element.

Figure 6. - Sketches of type 2 flame holding elements investigated. (All dimensions in inches.)

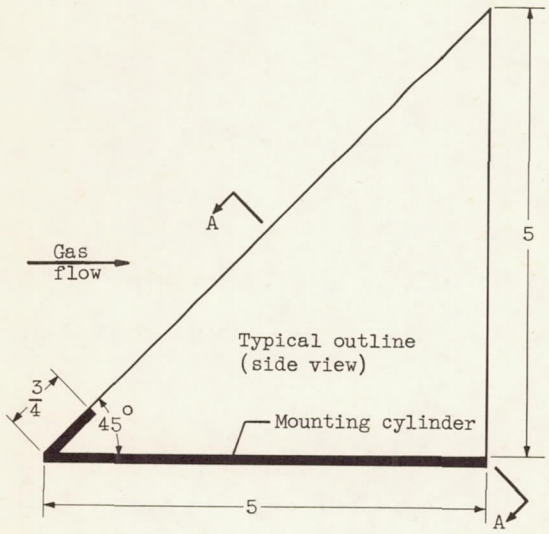

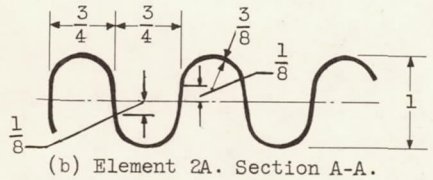

(b) Element 2A. Section A-A.

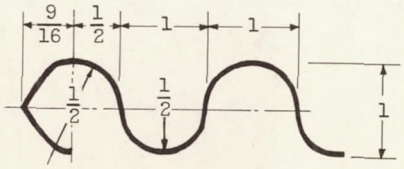

(c) Element 2B. Section A-A.

CD-3988

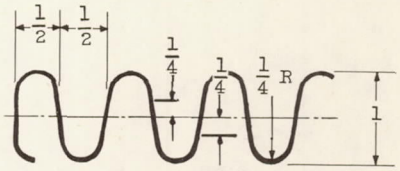

(d) Element 2C. Section A-A.

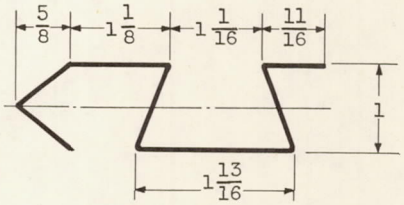

(e) Element 2D. Section A-A.

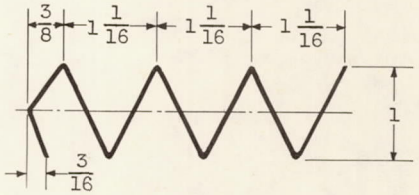

(f) Element 2E. Section A-A.

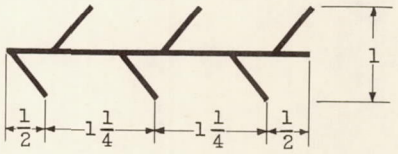

(g) Element 2F. Section A-A.

Figure 6. - Concluded. Sketches of type 2 flame holding elements investigated. (All dimensions in inches.)

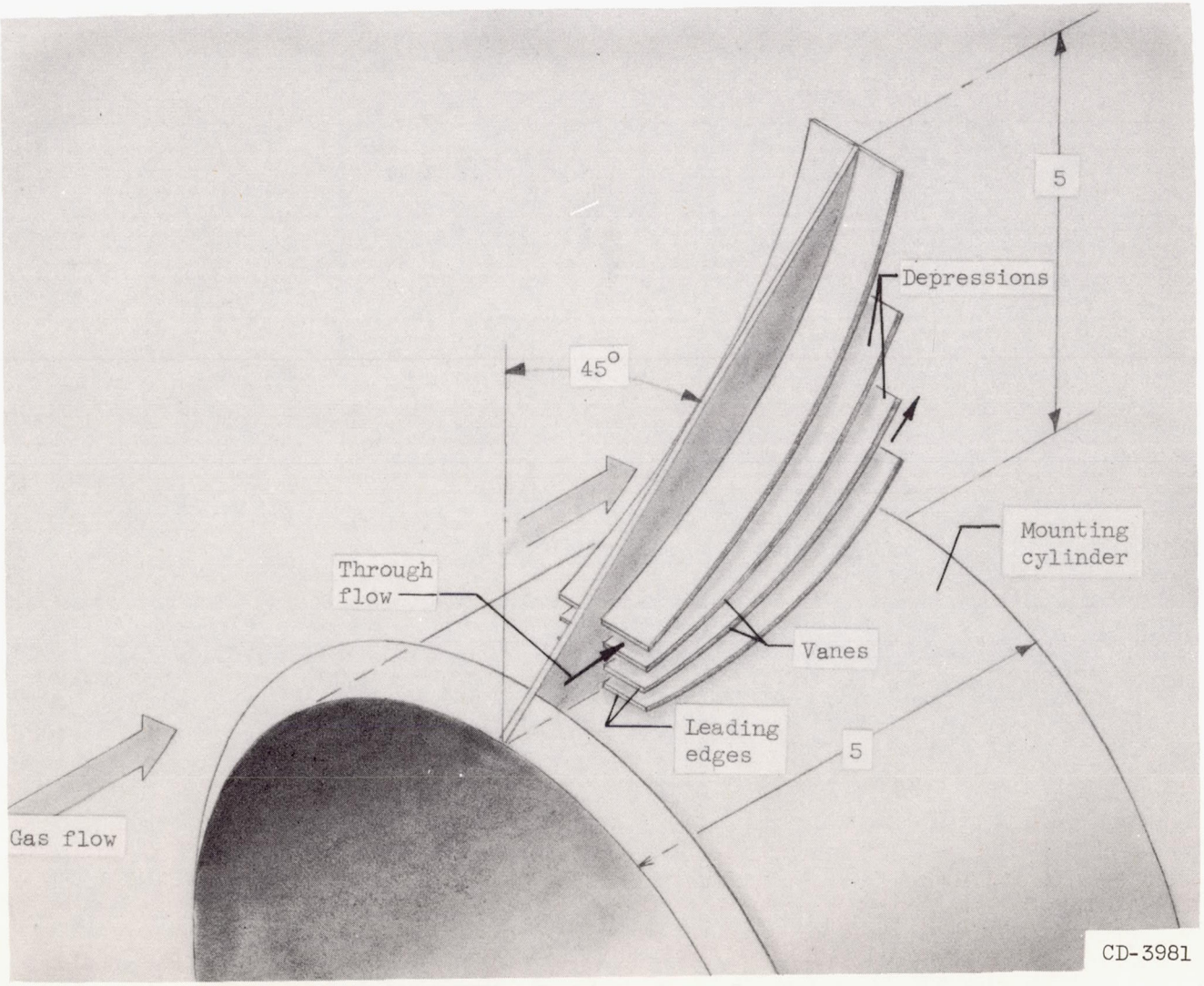

(a) Type 3 flame holder element.

Figure 7. - Sketches of type 3 flame holding element investigated. (All dimensions in inches.)

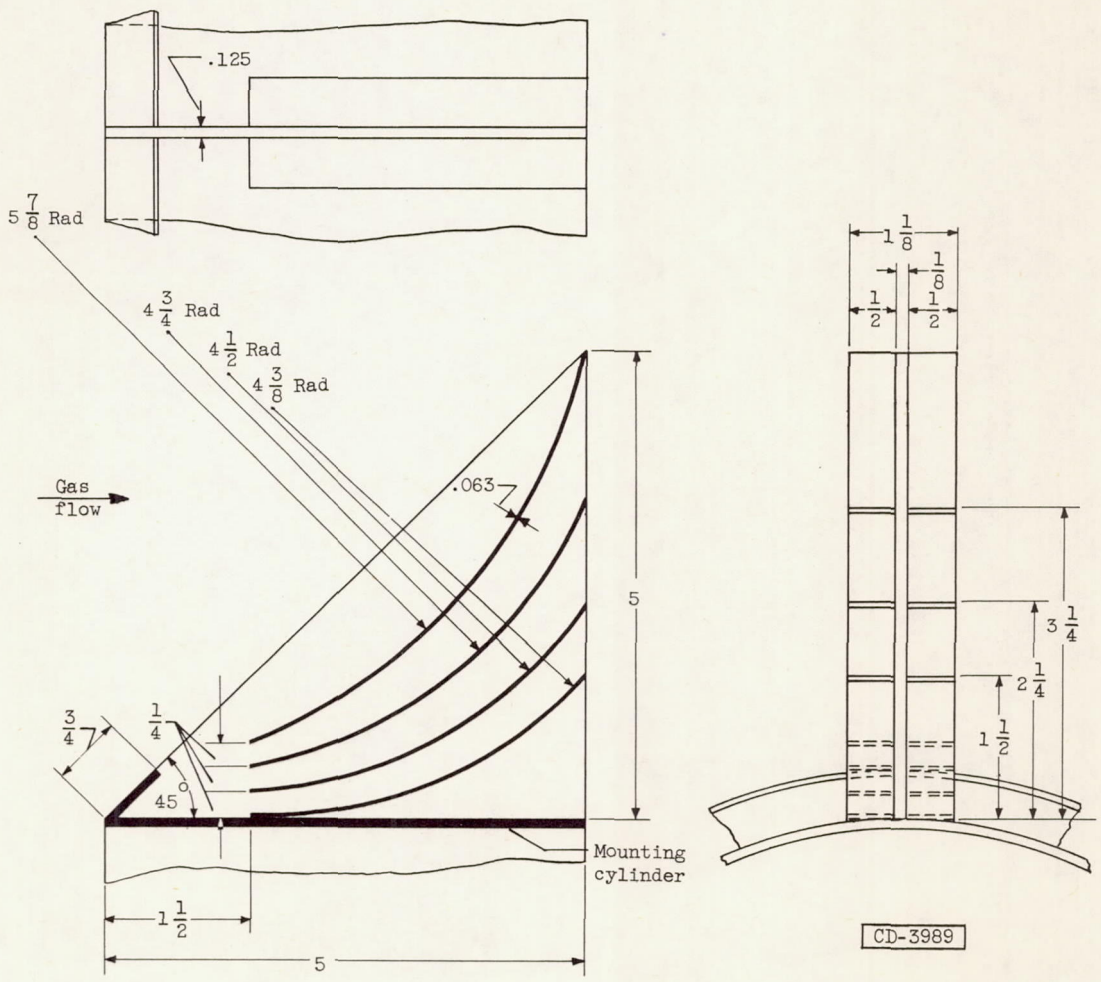

(b) Element 3A.

Figure 7. - Concluded. Sketch of type 3 flame holding element investigated. (All dimensions in inches.)

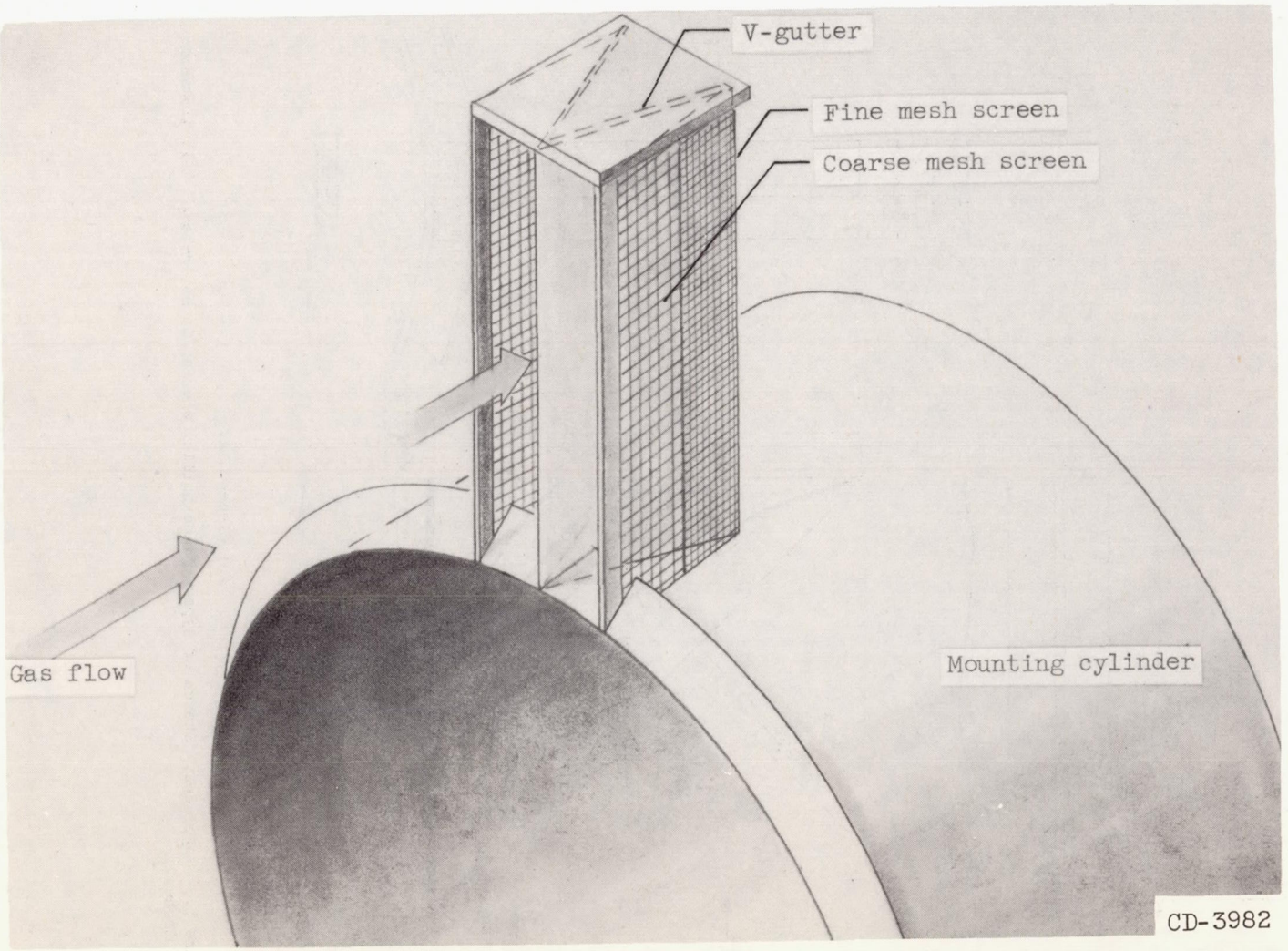

(a) Type 4 flame holder element; screens swept forward from trailing edge of V-gutter.

Figure 8. - Sketches of type 4 flame holding elements investigated. (All dimensions in inches.)

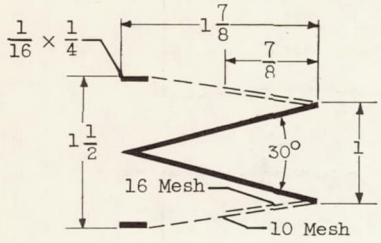

(b) Element 4A.

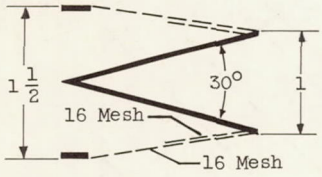

(c) Element 4B.

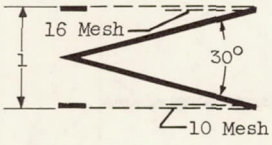

(d) Element 4C.

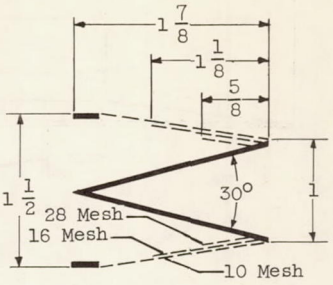

(e) Element 4D.

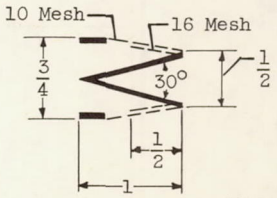

(f) Element 4E.

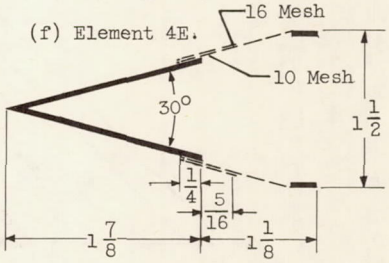

(g) Element 4F.

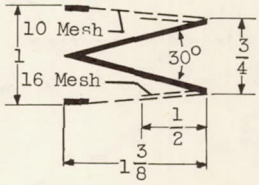

(h) Element 4G.

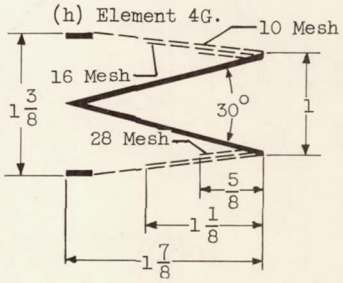

(m) Element 4L.

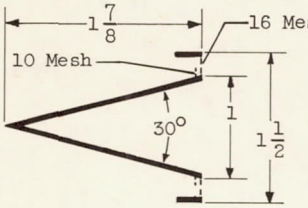

(k) Element 4J.

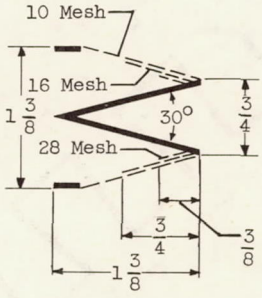

(l) Element 4K.

CD 3992

Figure 8. - Continued. Sketches of type 4 flame holding elements investigated. (All dimensions in inches.)

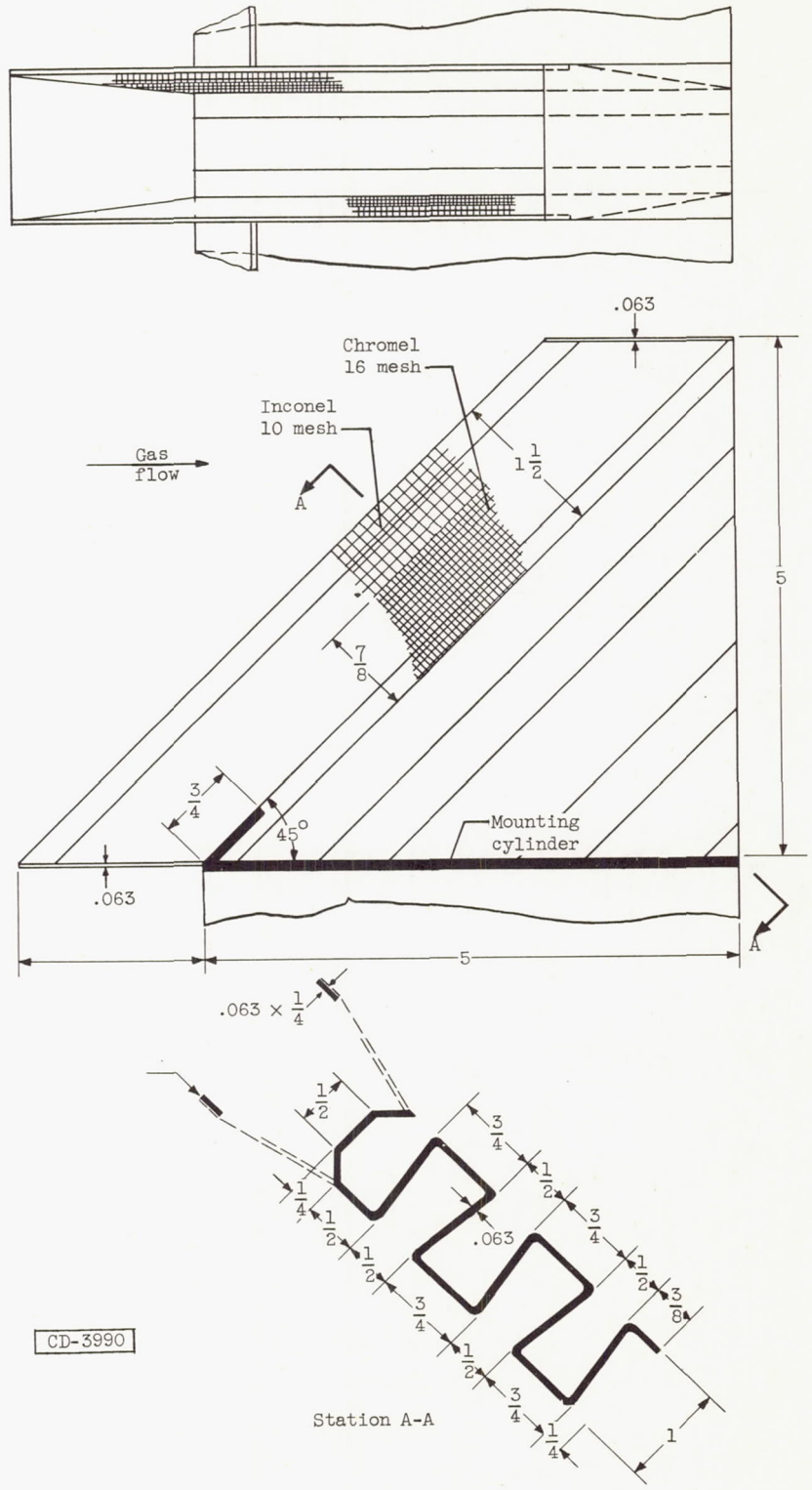

(i) Element 4H.

Figure 8. - Continued. Sketches of type 4 flame holding elements investigated. (All dimensions in inches.)

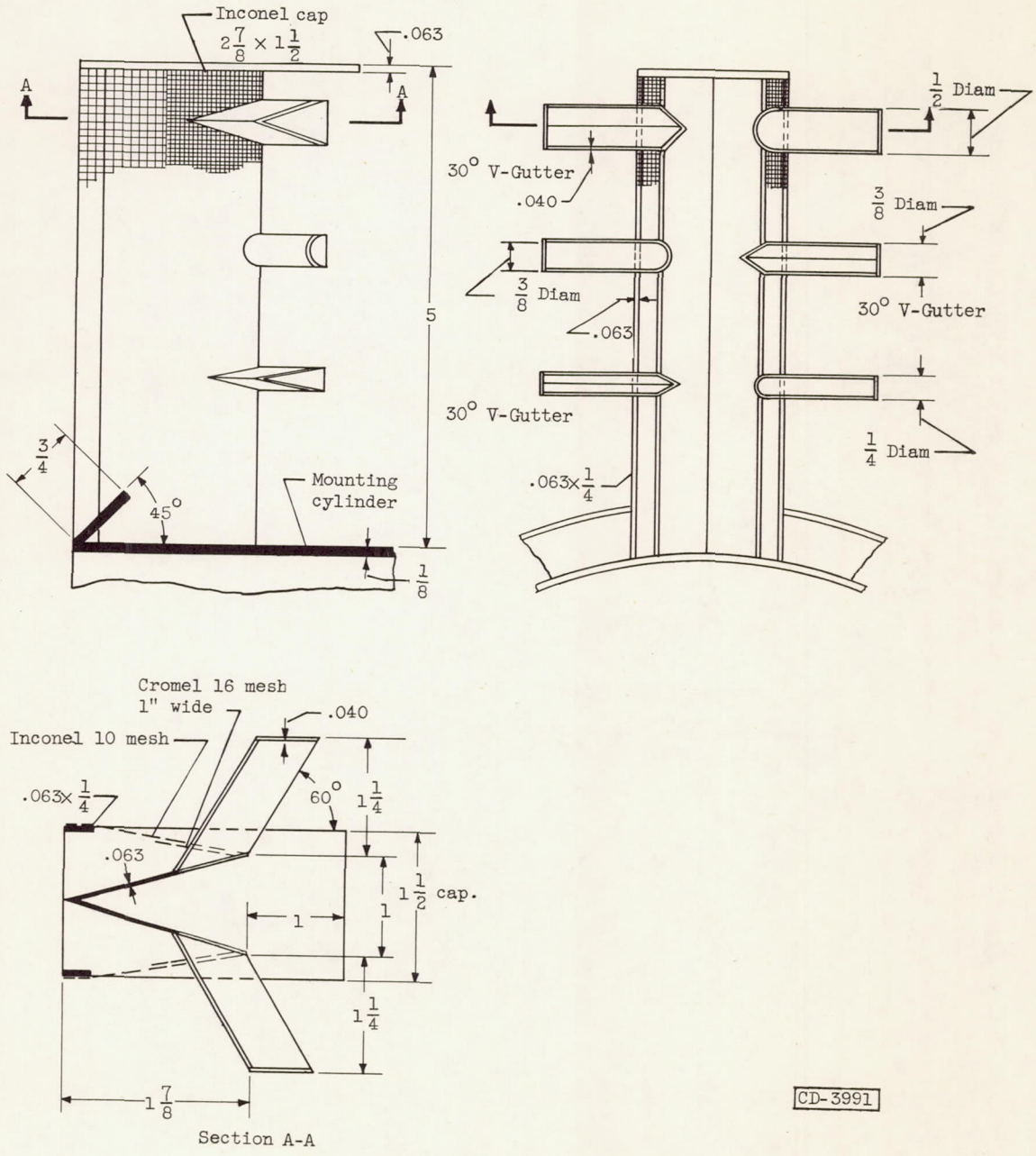

(j) Element 4I.

Figure 8. - Concluded. Sketches of type 4 flame holding elements investigated. (All dimensions in inches.)

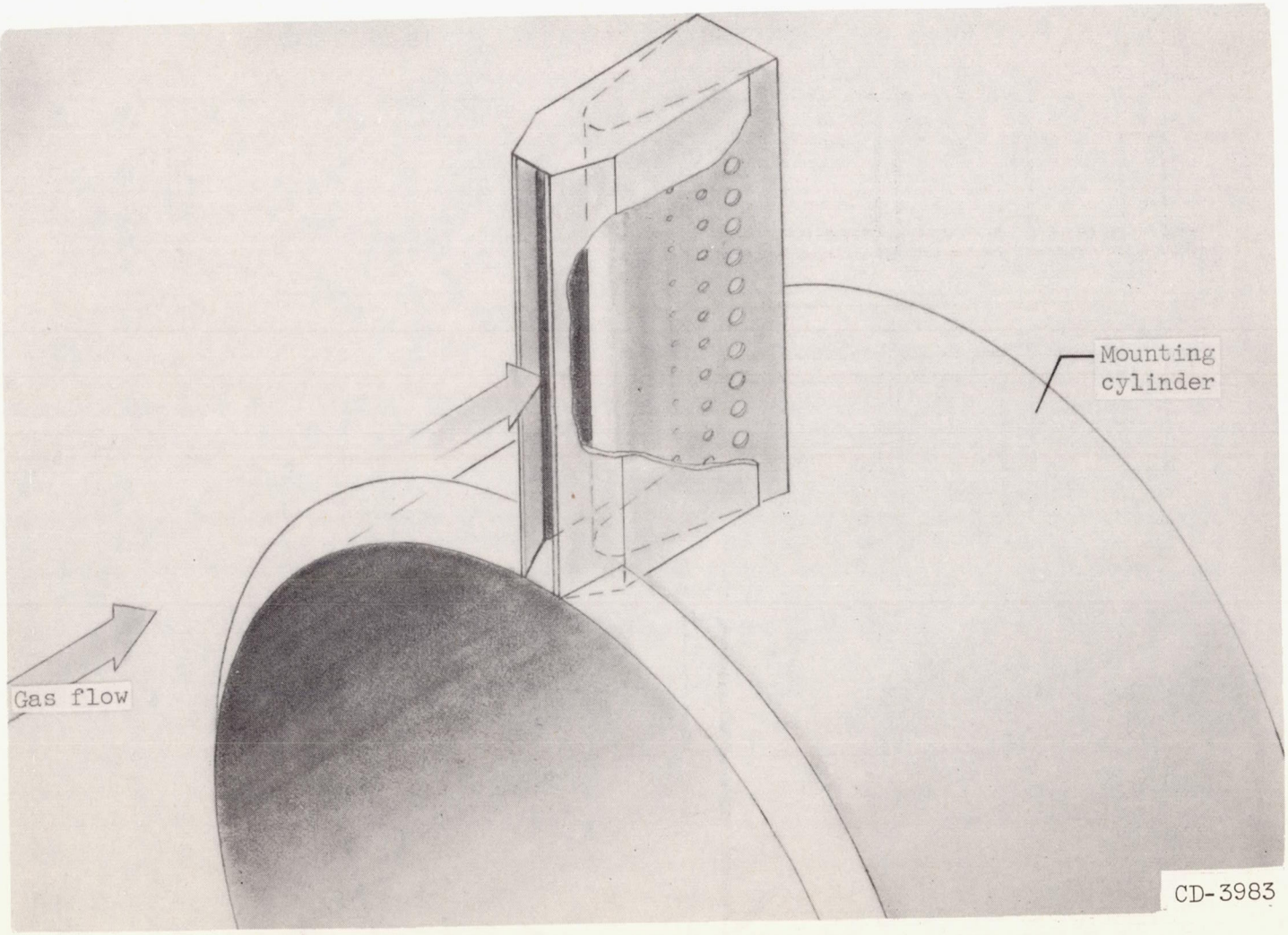

(a) Type 5 flame holder element.

Figure 9. - Sketches of type 5 flame holding elements investigated. (All dimensions in inches.)

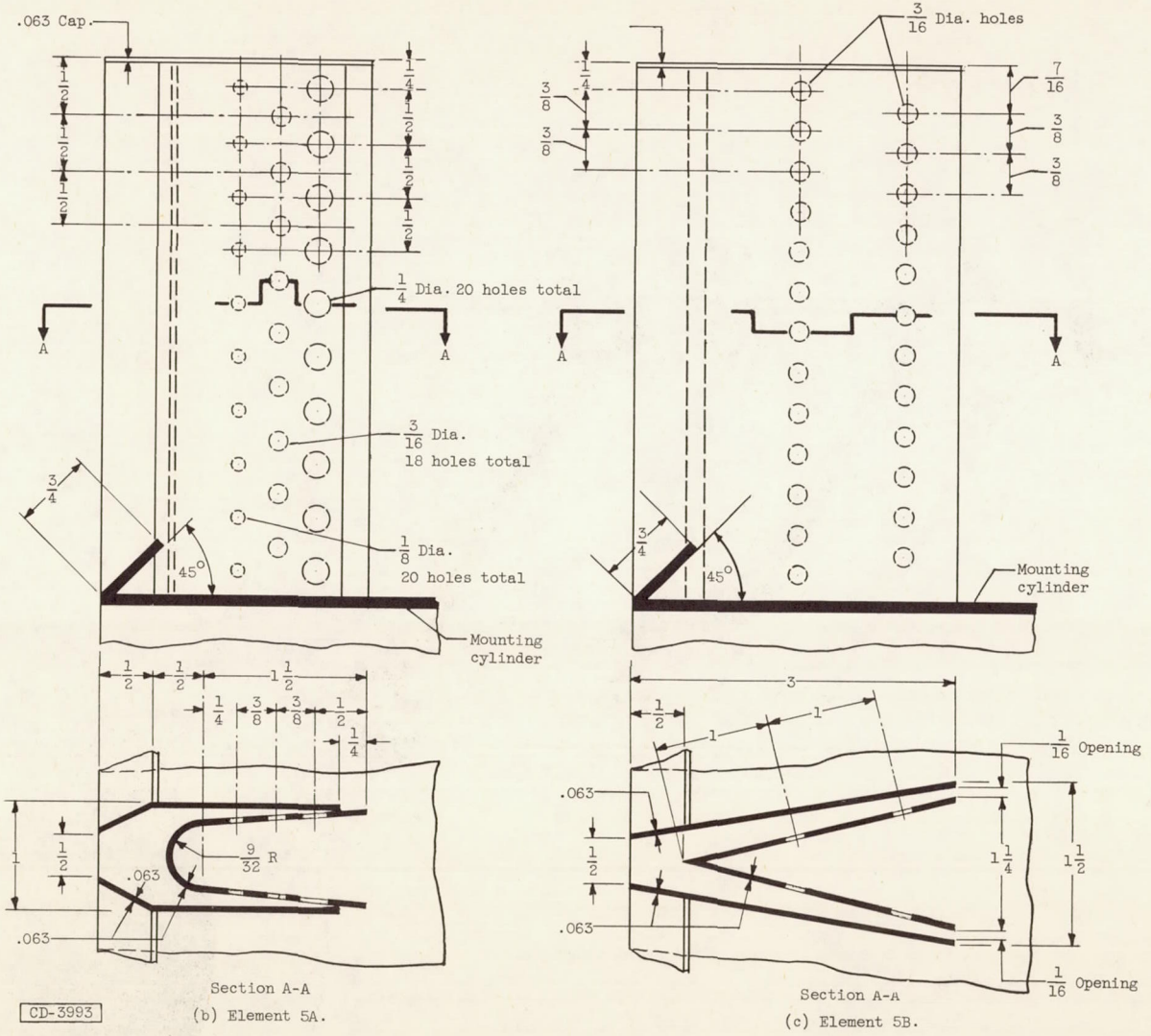

Figure 9. - Concluded. Sketches of type 5 flame holding elements investigated. (All dimensions in inches.)

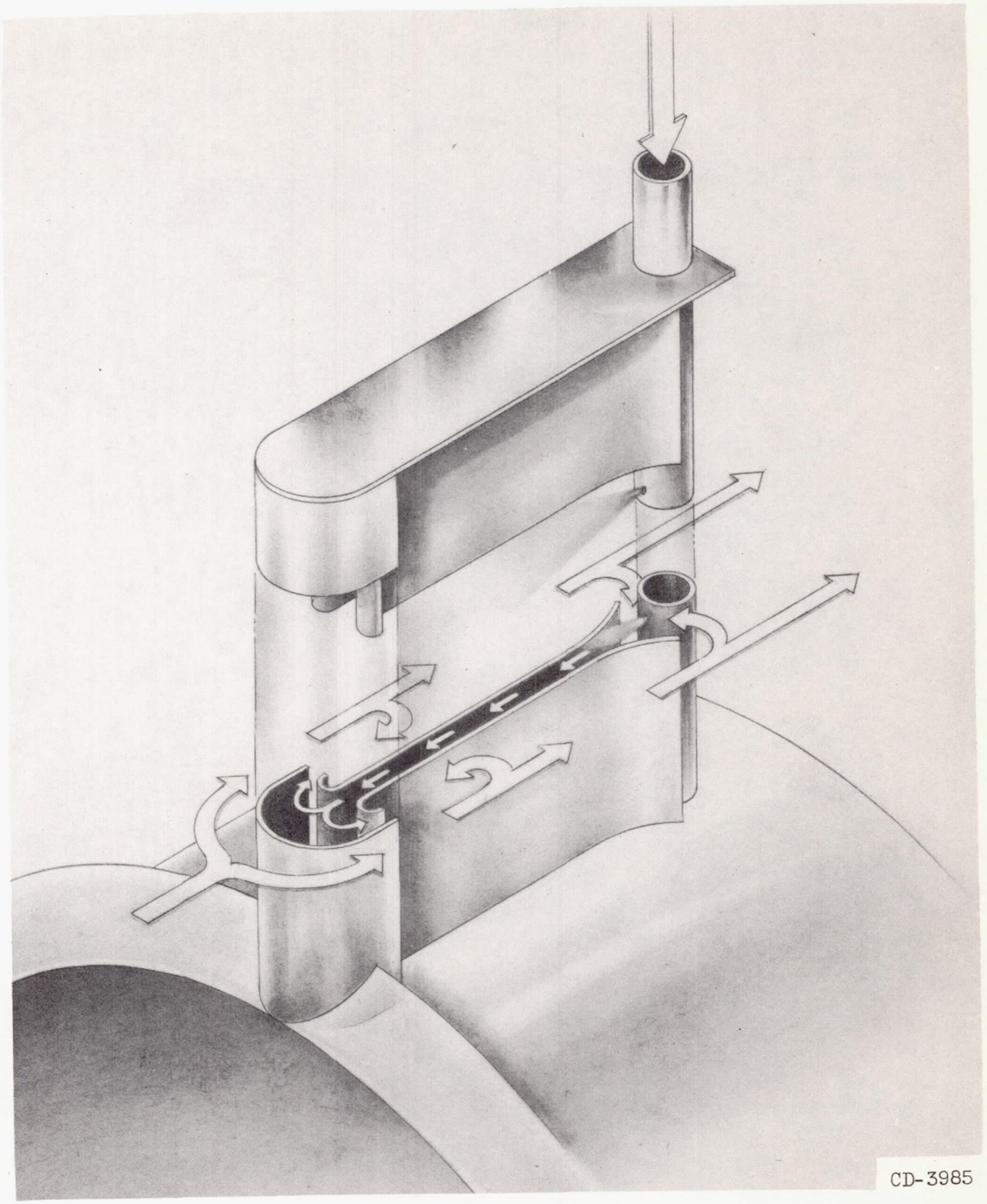

(a) Cutaway view of type 6 flame holding element.

Figure 10. - Sketches of type 6 flame holding elements investigated. (All dimensions in inches.)

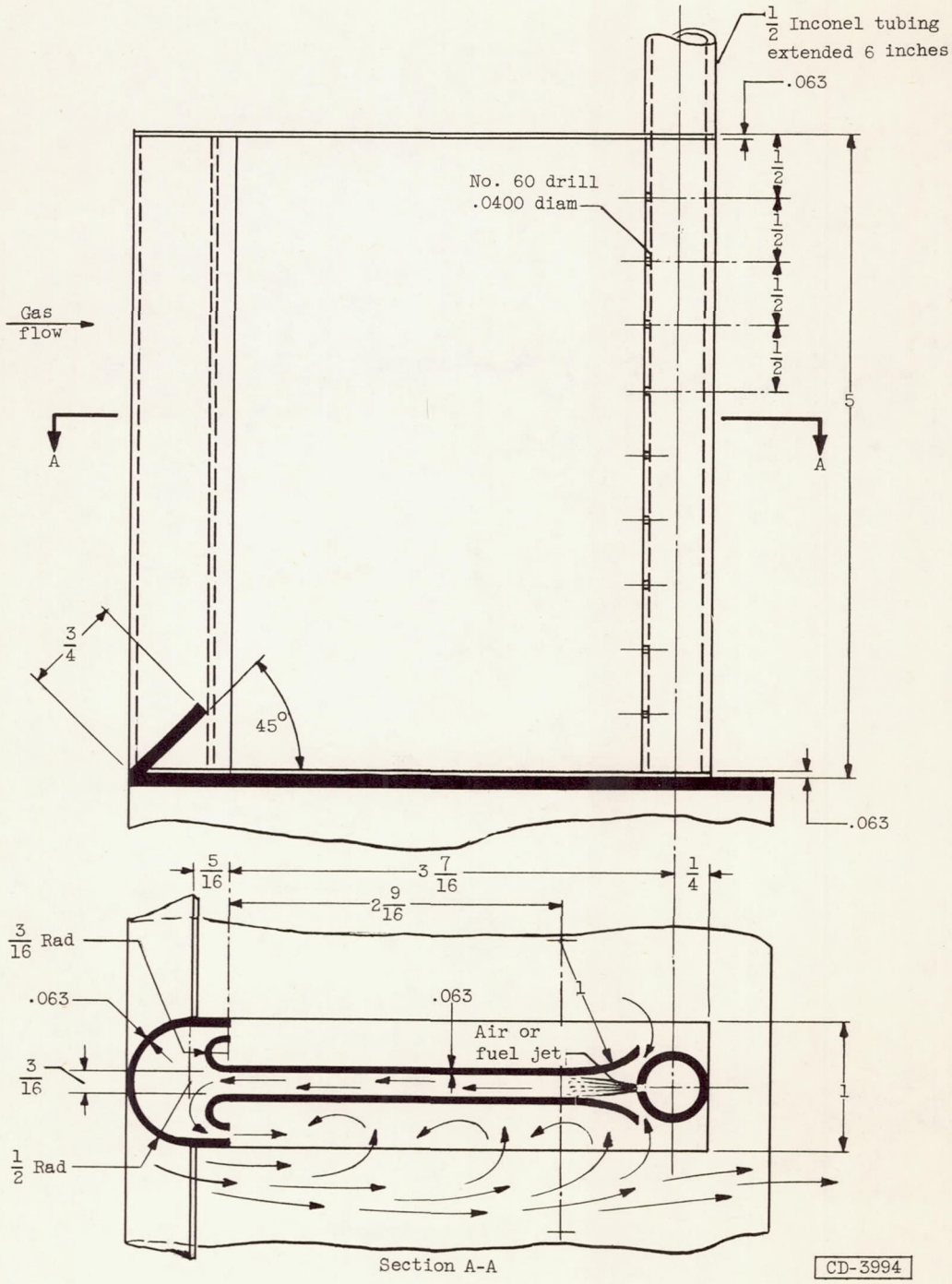

(b) Element 6A.

Figure 10. - Sketches of type 6 flame holding element investigated. (All dimensions in inches.)

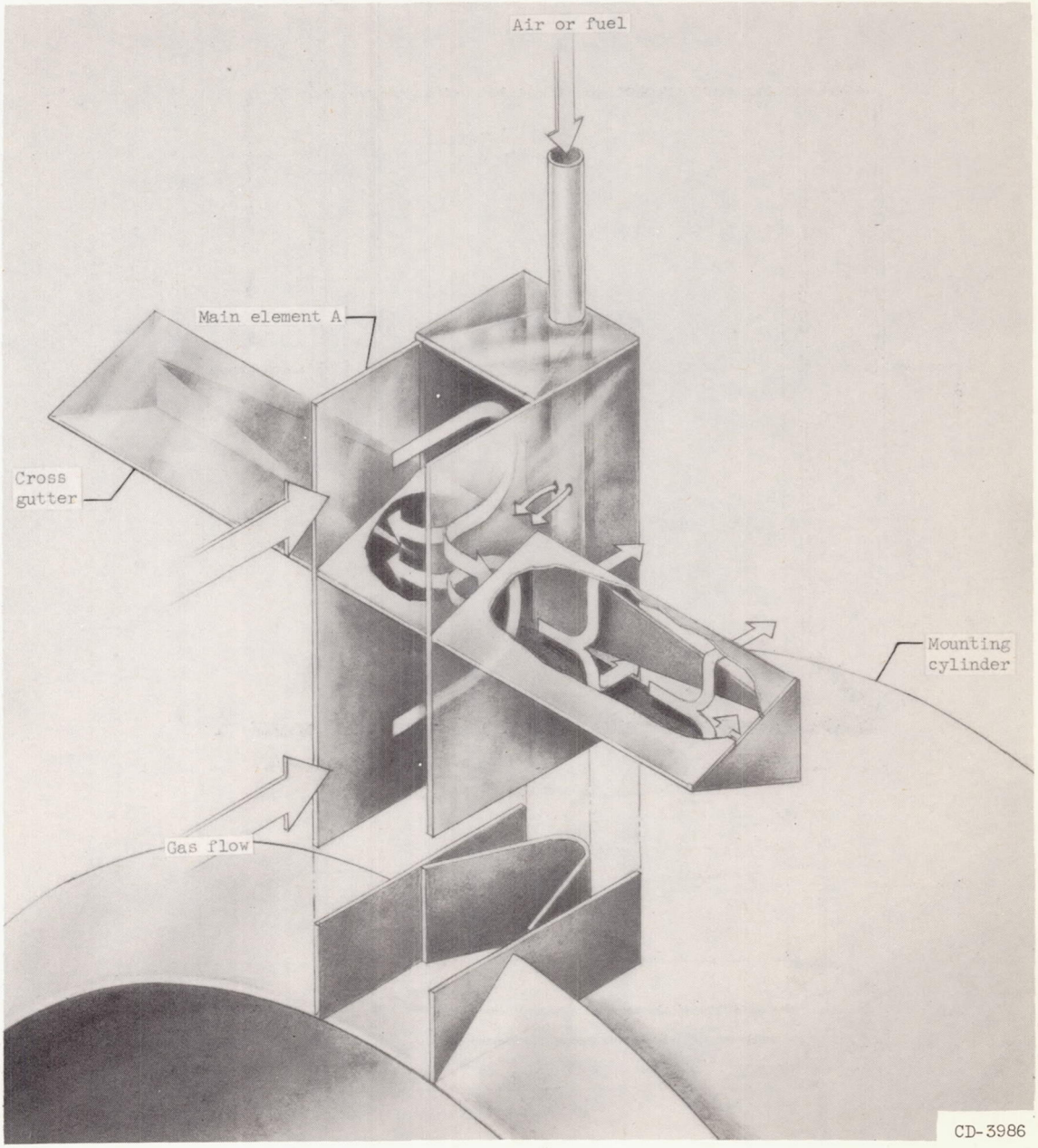

(a) Type 7 flame holder element.

Figure 11. - Sketches of type 7 flame holding elements investigated. (All dimensions in inches.)

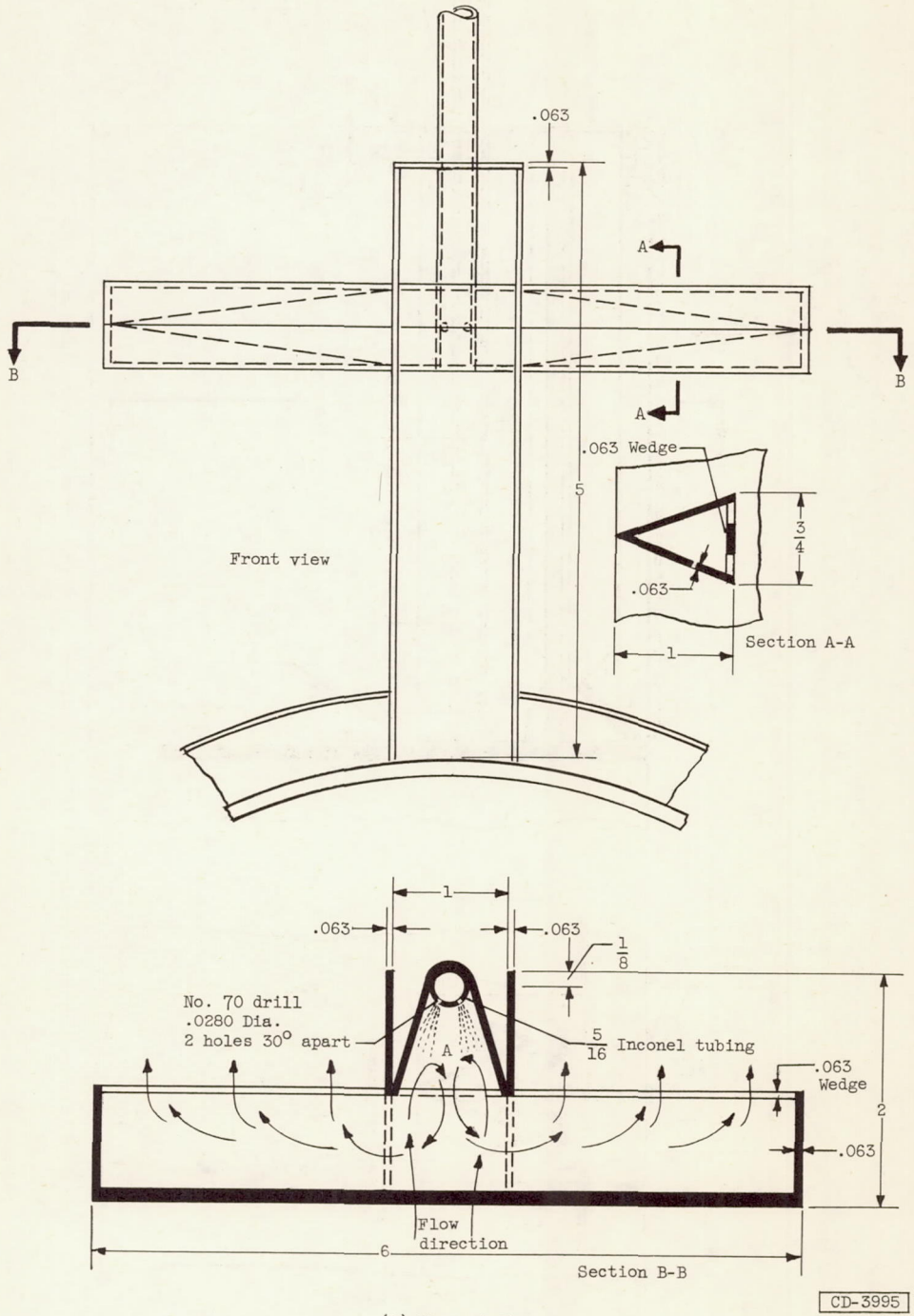

(b) Element 7A.

Figure 11. - Continued. Sketches of type 7 flame holding elements investigated. (All dimensions in inches.)

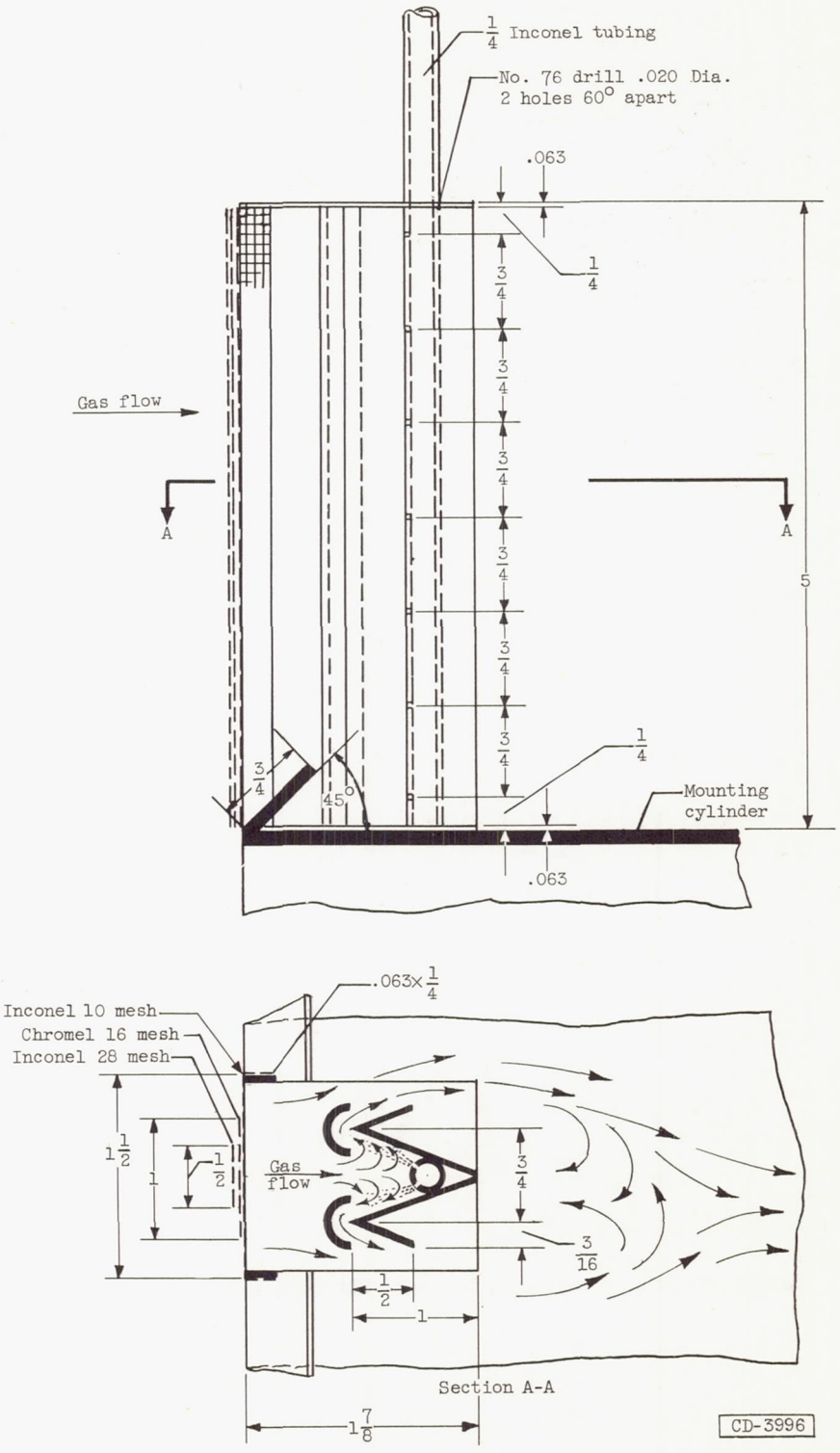

(c) Element 7B.

Figure 11. - Continued. Sketches of type 7 flame holding elements investigated. (All dimensions in inches.)

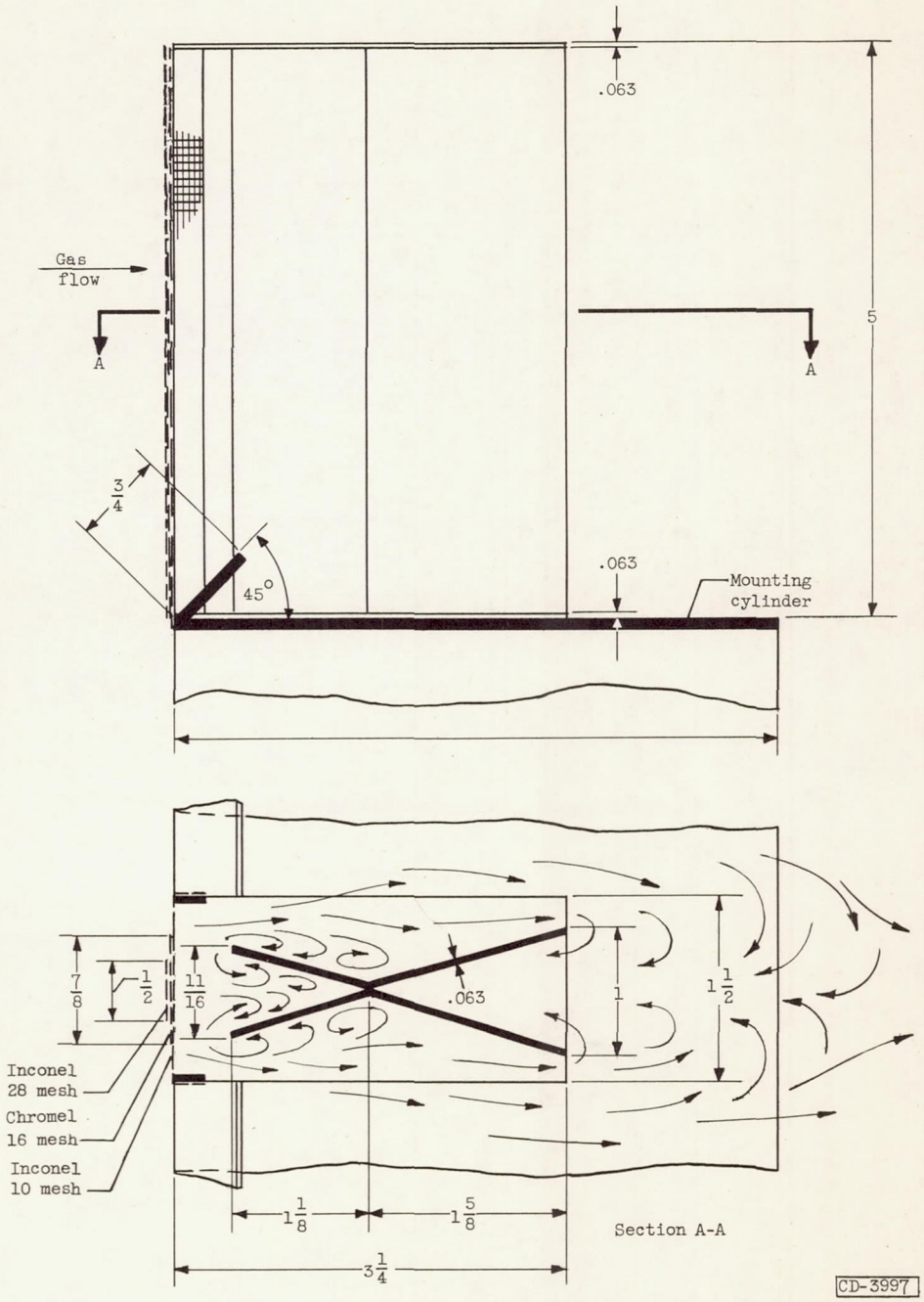

(d) Element 7C.

Figure 11. - Continued. Sketches of type 7 flame holding elements investigated. (All dimensions in inches.)

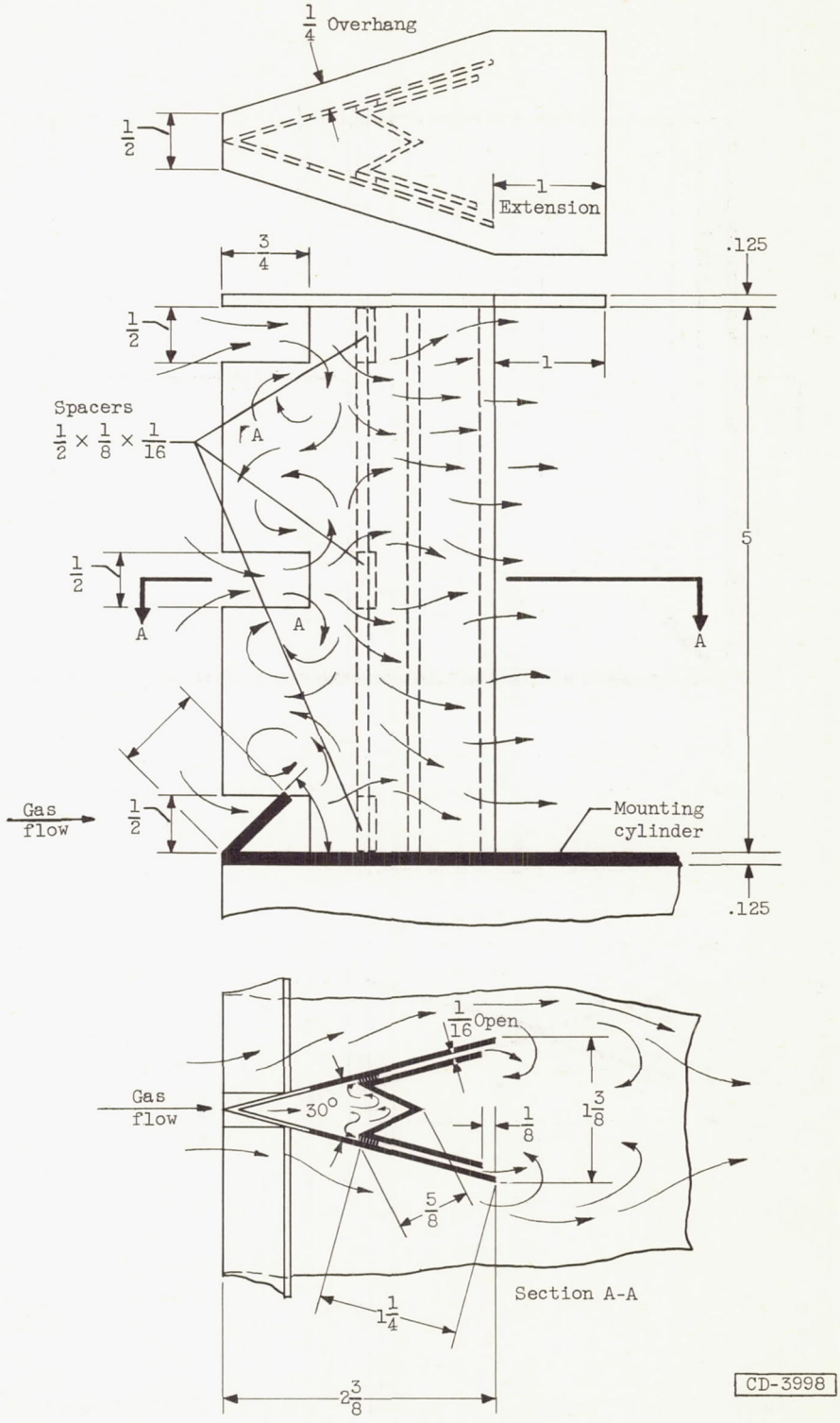

(e) Element 7D.

Figure 11. - Concluded. Sketches of type 7 flame holding elements investigated. (All dimensions in inches.)

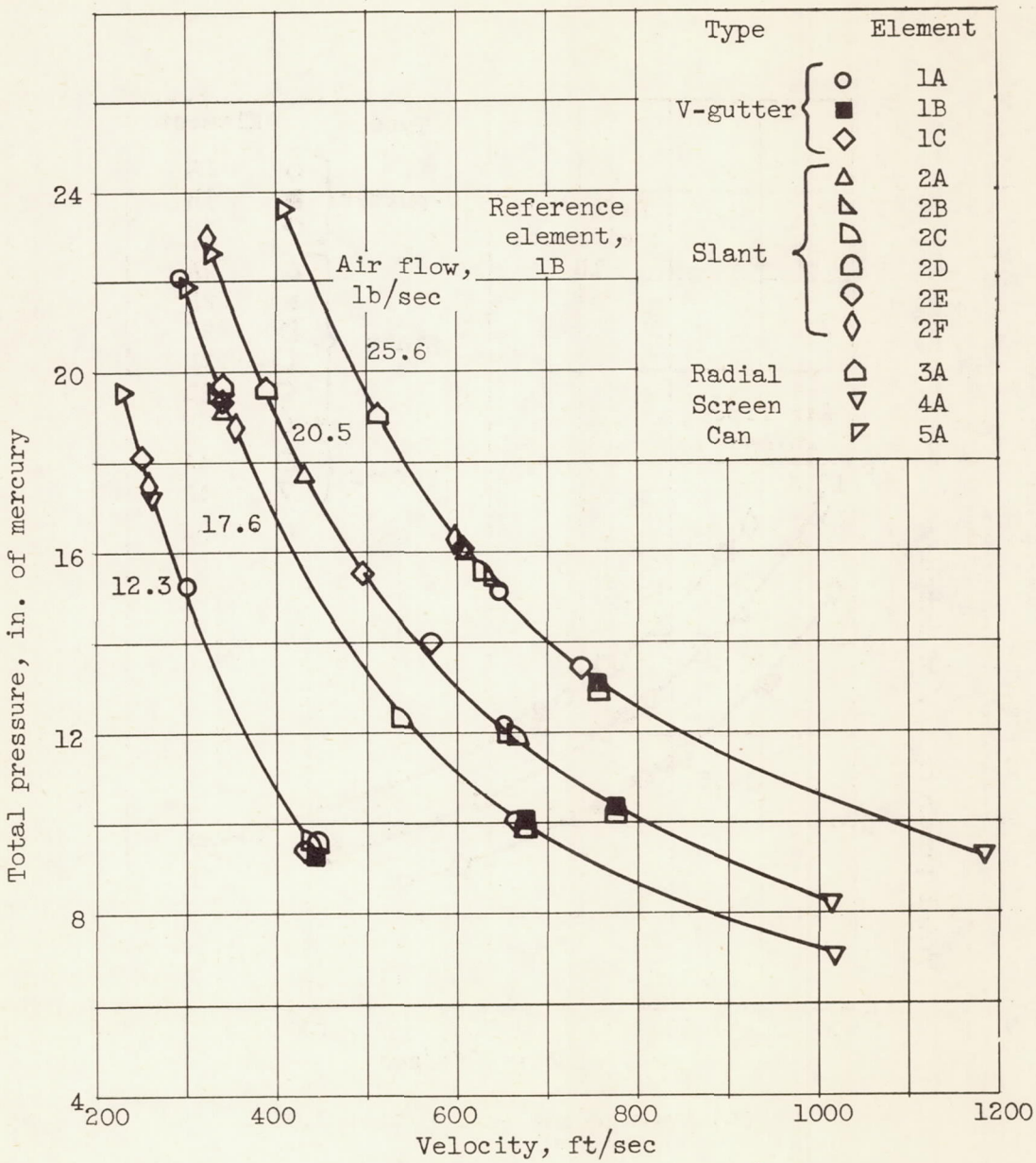

(a) Average fuel-air ratio, 0.0405.

Figure 12. - Stability limits of elements in number 1 assembly.

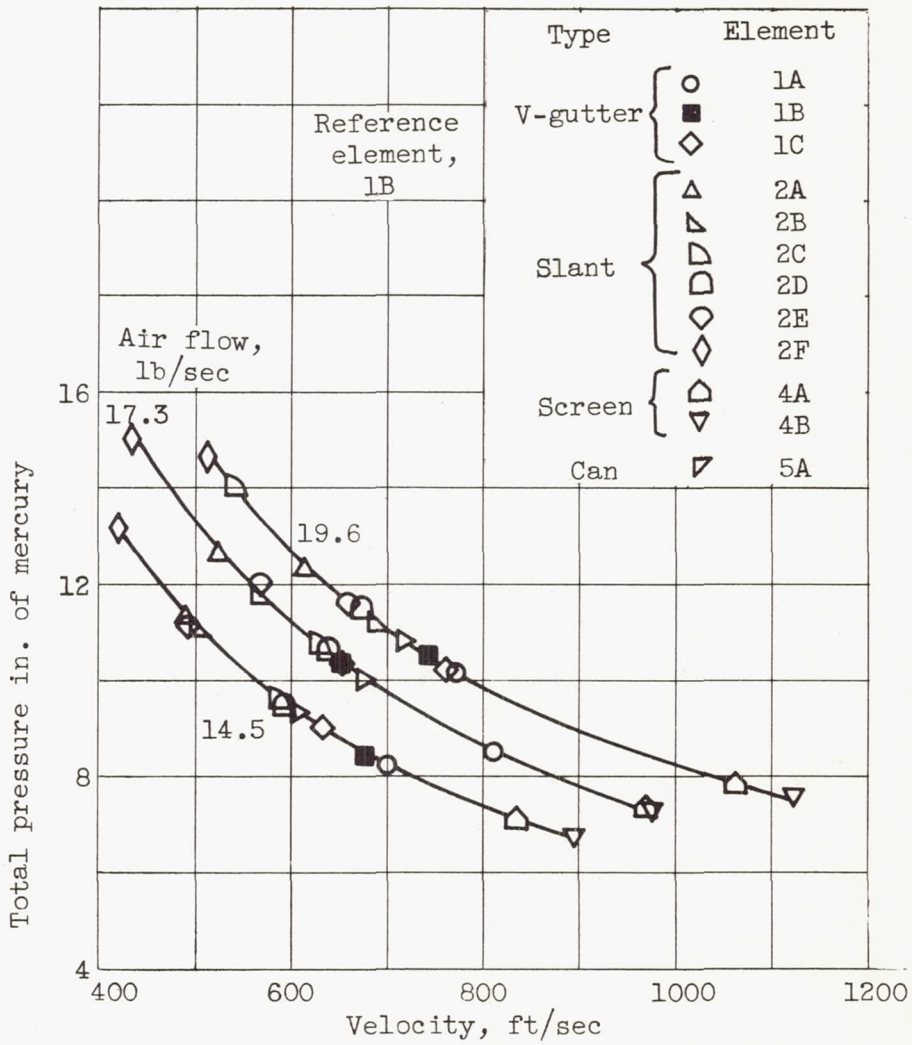

(b) Average fuel-air ratio, 0.038.

Figure 12. - Continued. Stability limits of elements in number 1 assembly.

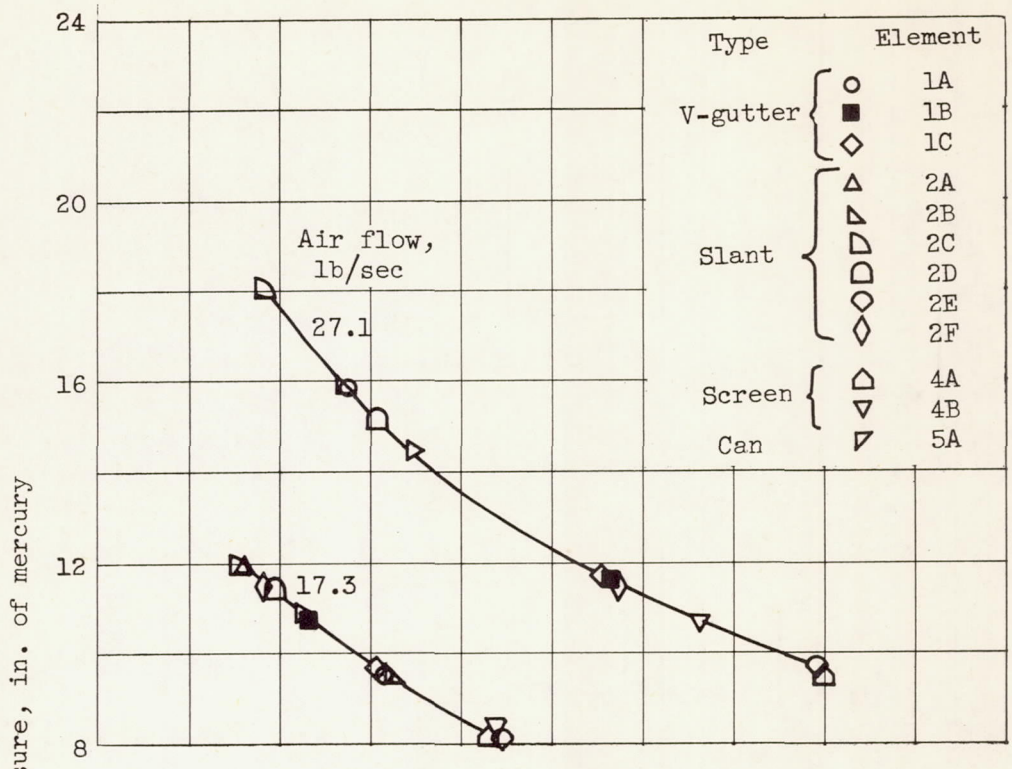

(c) Average fuel-air ratio, 0.045.

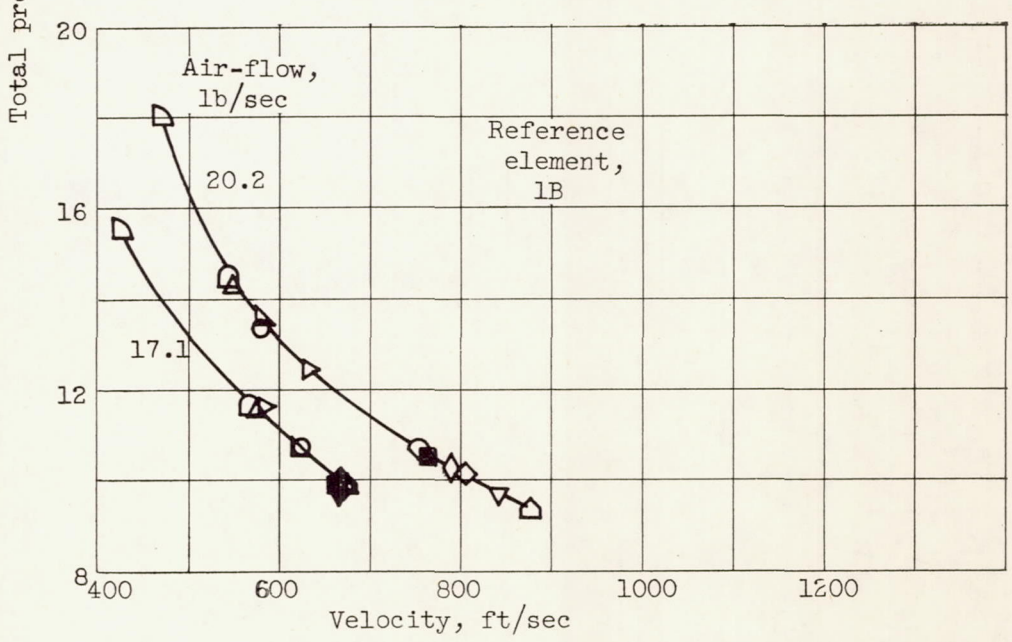

(d) Average fuel-air ratio, 0.0515.

Figure 12. - Concluded. Stability limits of elements in number 1 assembly.

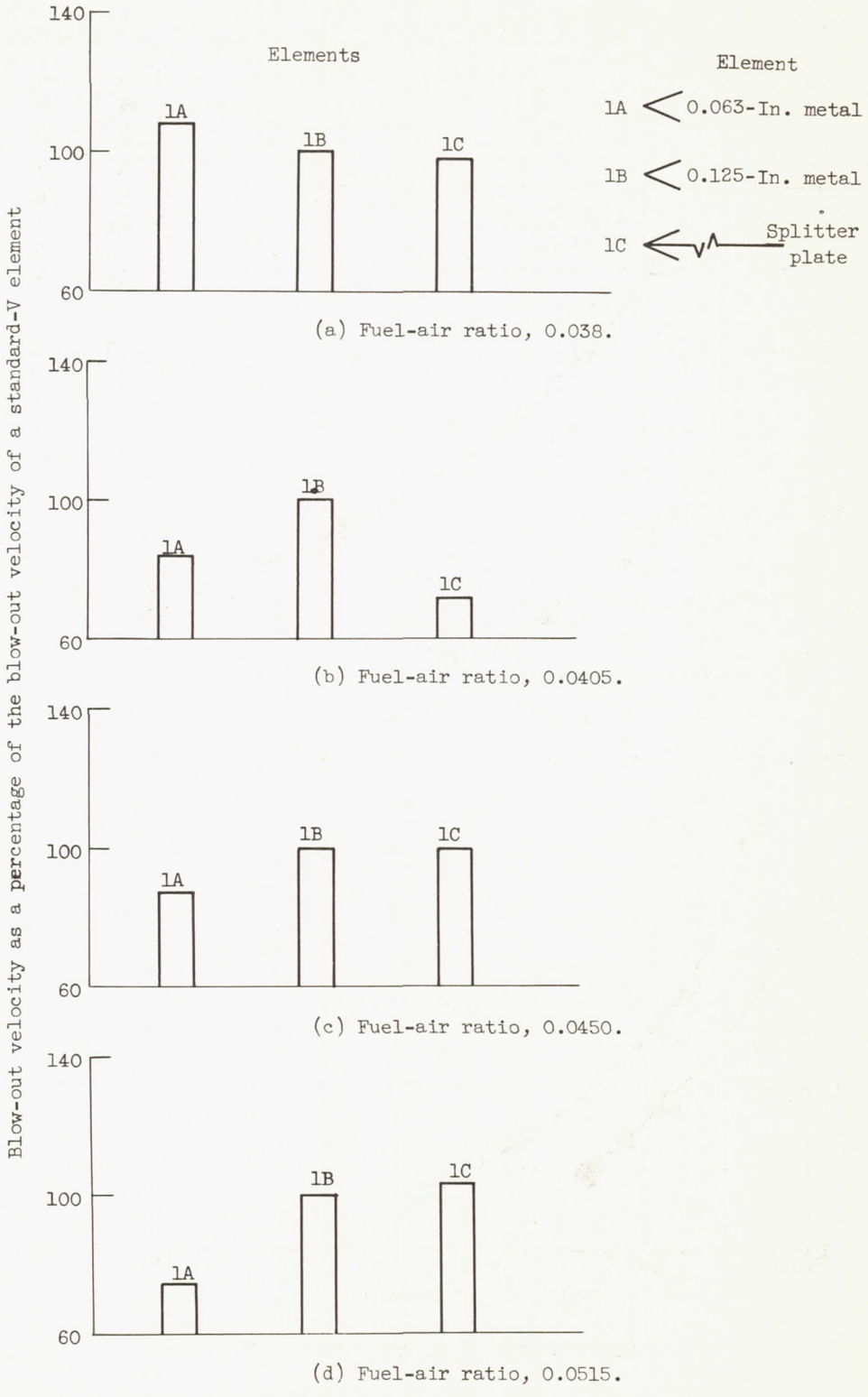

Figure 13. - Relative performance of type 1 elements in assembly number 1.

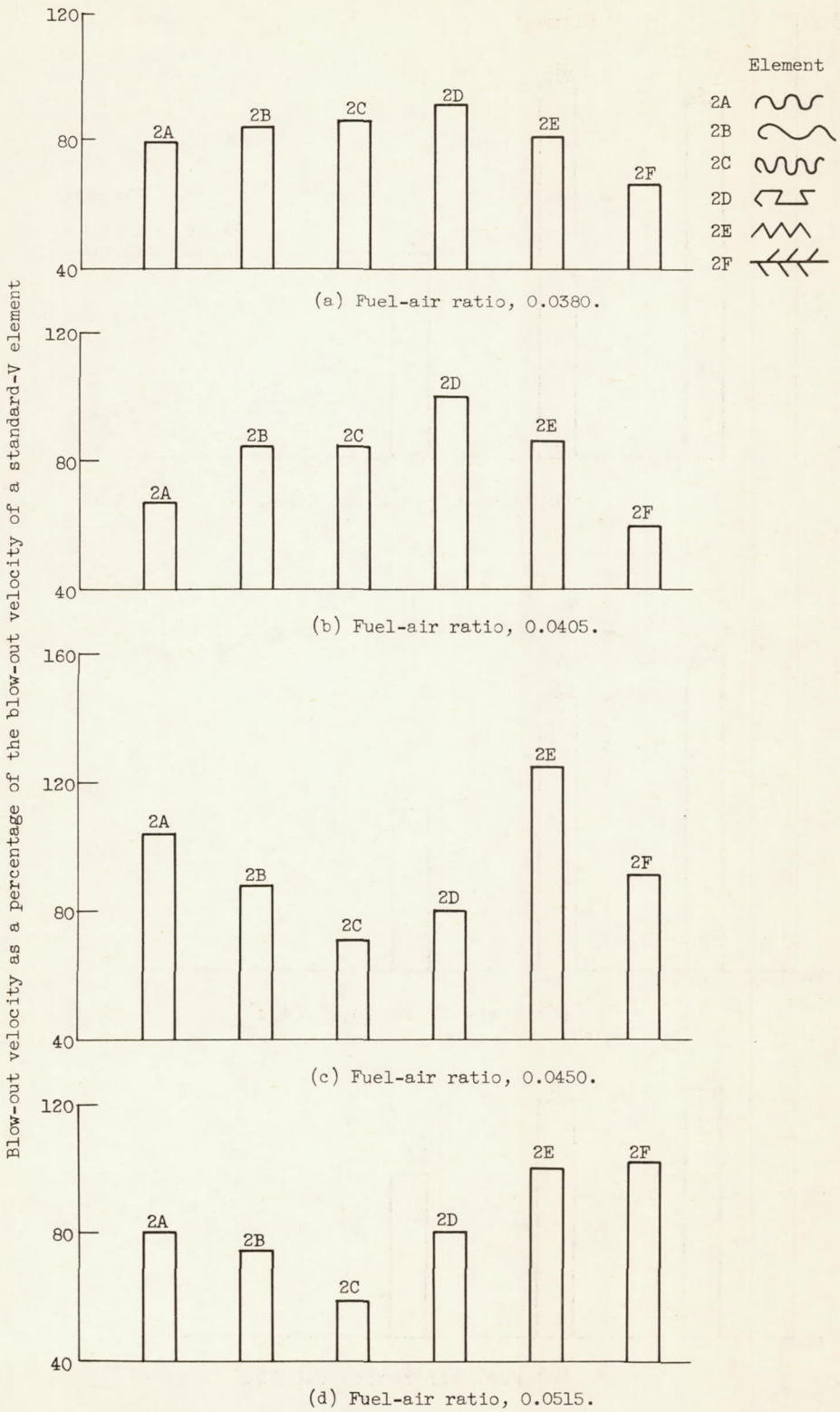

Figure 14. - Relative performance of type 2 elements in assembly number 1.

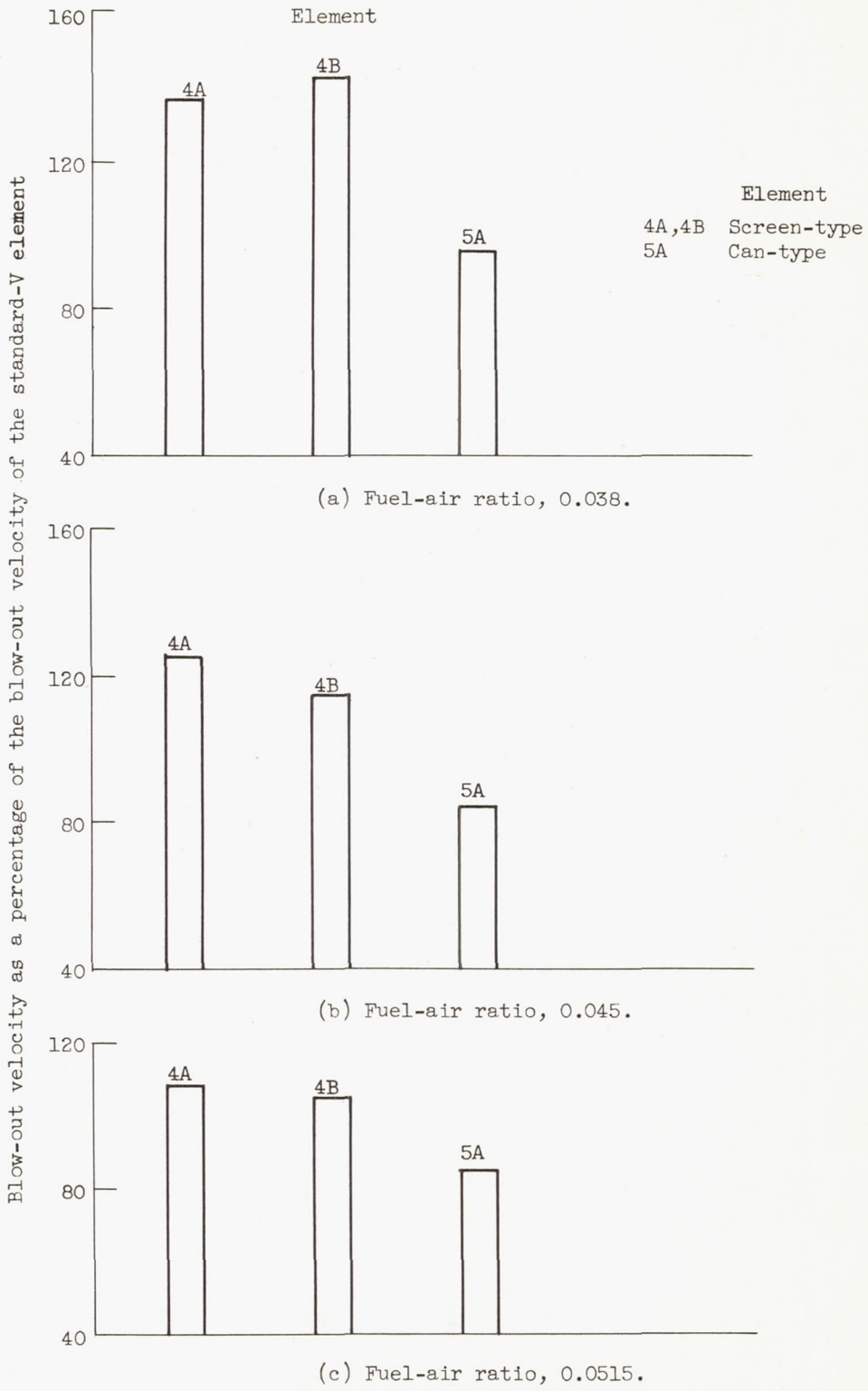

Figure 15. - Relative performance of type 4 and 5 elements in assembly number 1.

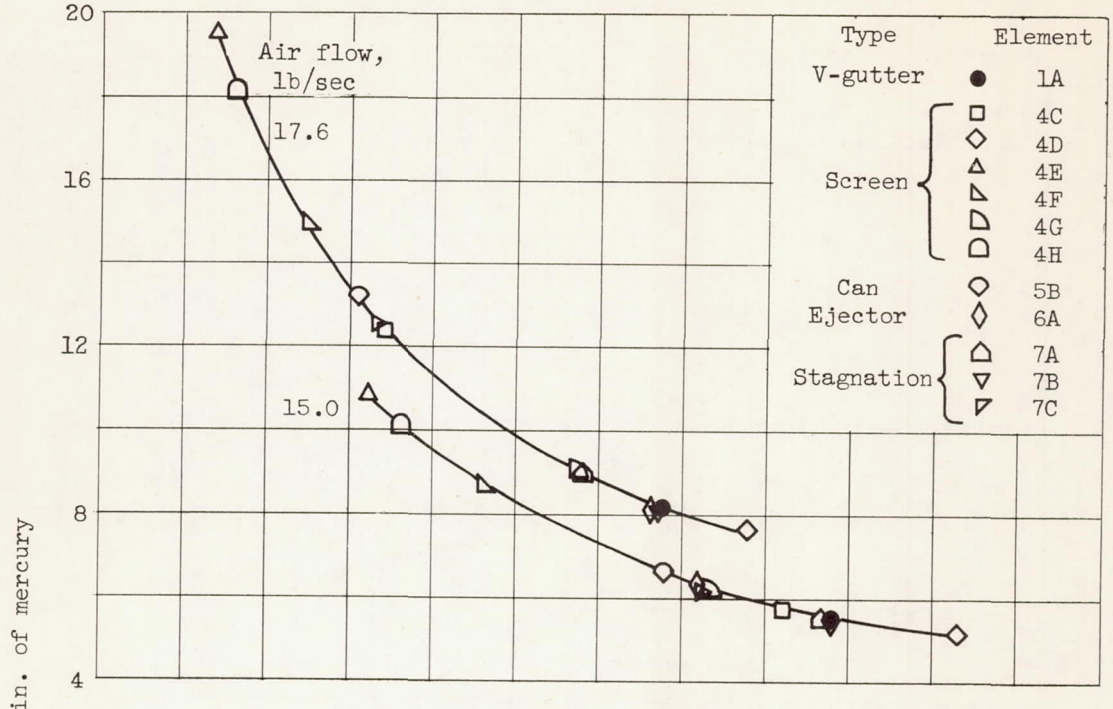

(a) Average fuel-air ratio, 0.024.

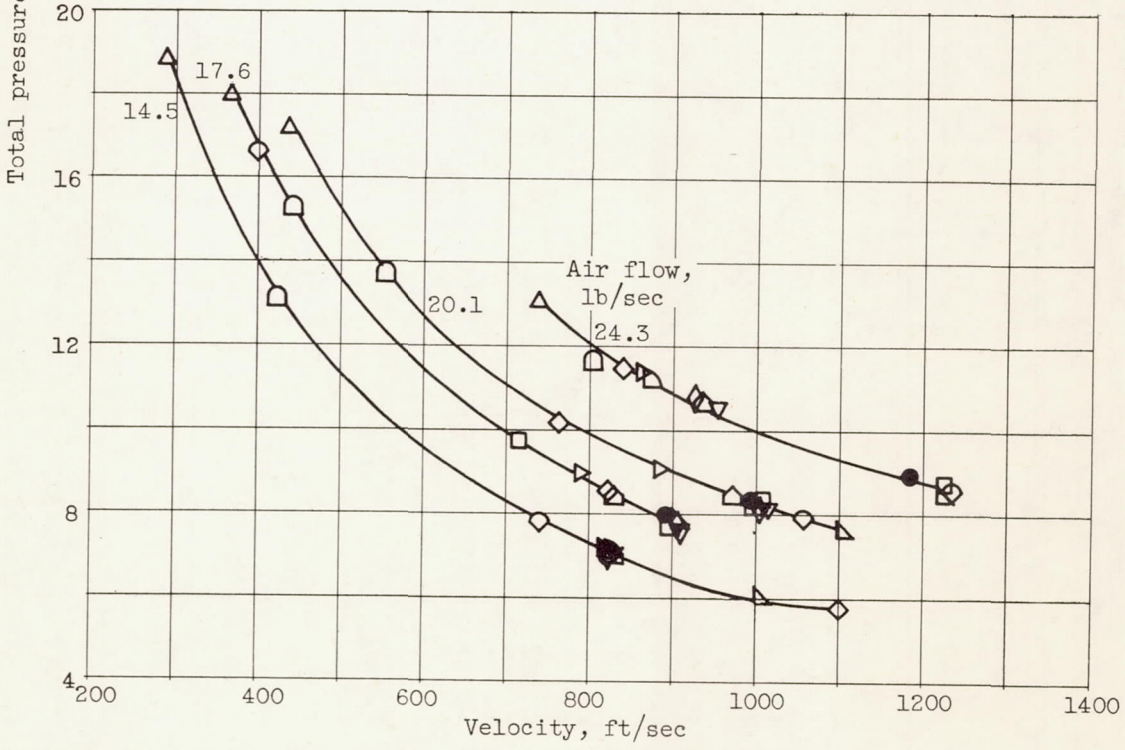

(b) Average fuel-air ratio, 0.037.

Figure 16. - Stability limits of elements in number 2 assembly.

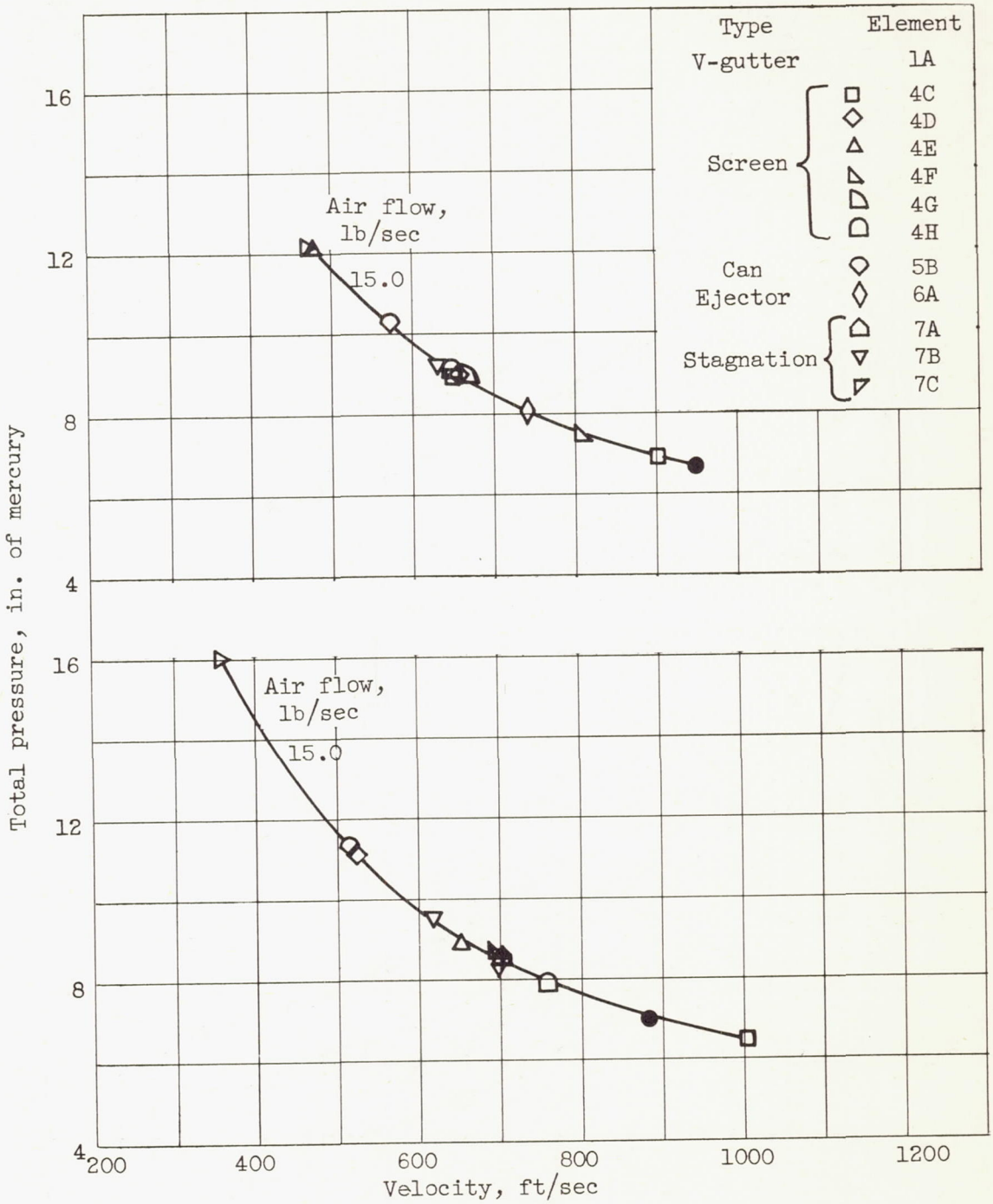

(c) Average fuel-air ratio, 0.0505.

Figure 16. - Continued. Stability limits of elements in number 2 assembly.

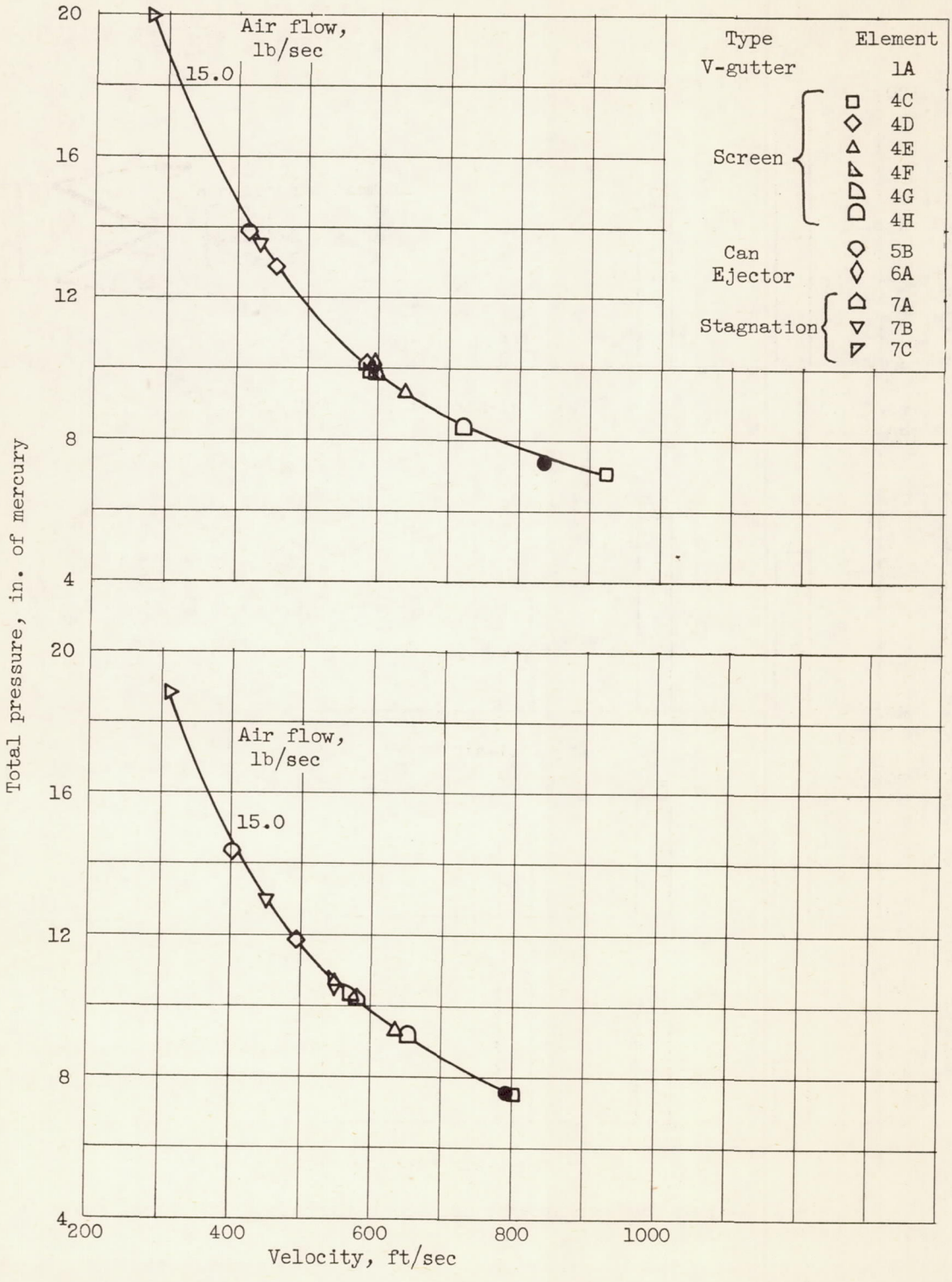

(d) Average fuel-air ratio, 0.0625.

Figure 16. - Concluded. Stability limits of elements in number 2 assembly.

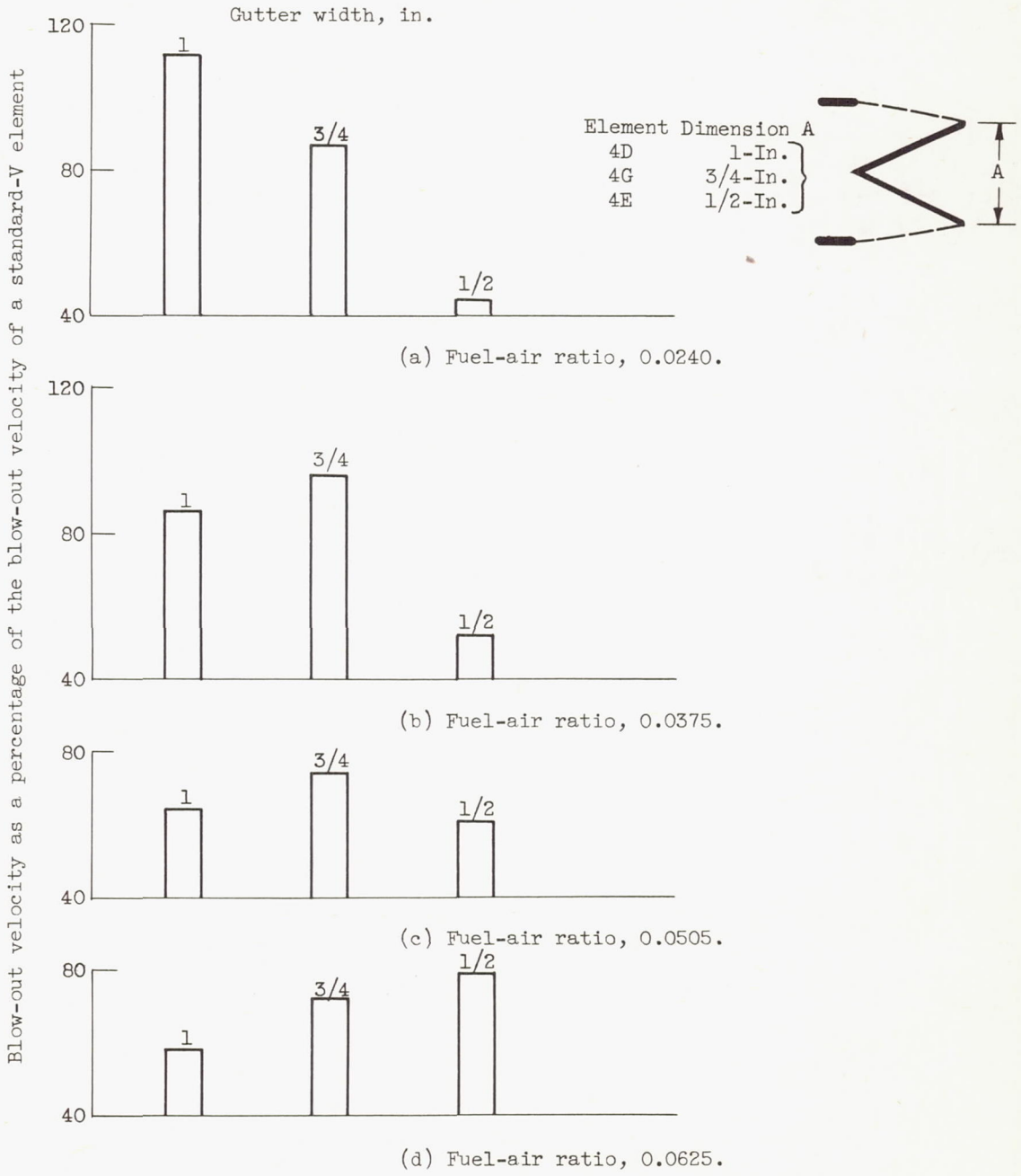

Figure 17. - Relative performance of type 4 elements of different scale in assembly number 2.

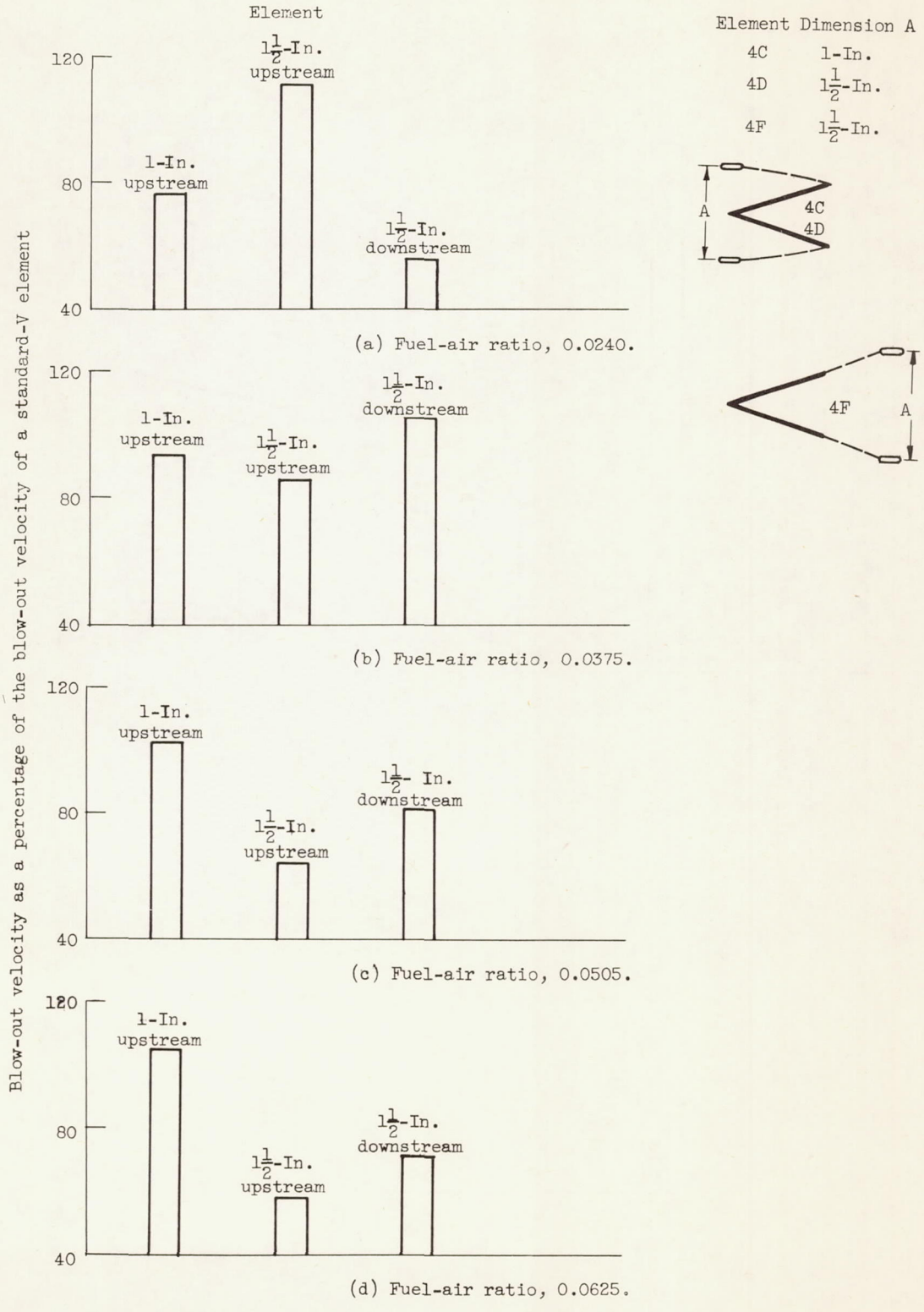

Figure 18. - Relative performance of type 4 elements of varied screen geometry in assembly number 2.

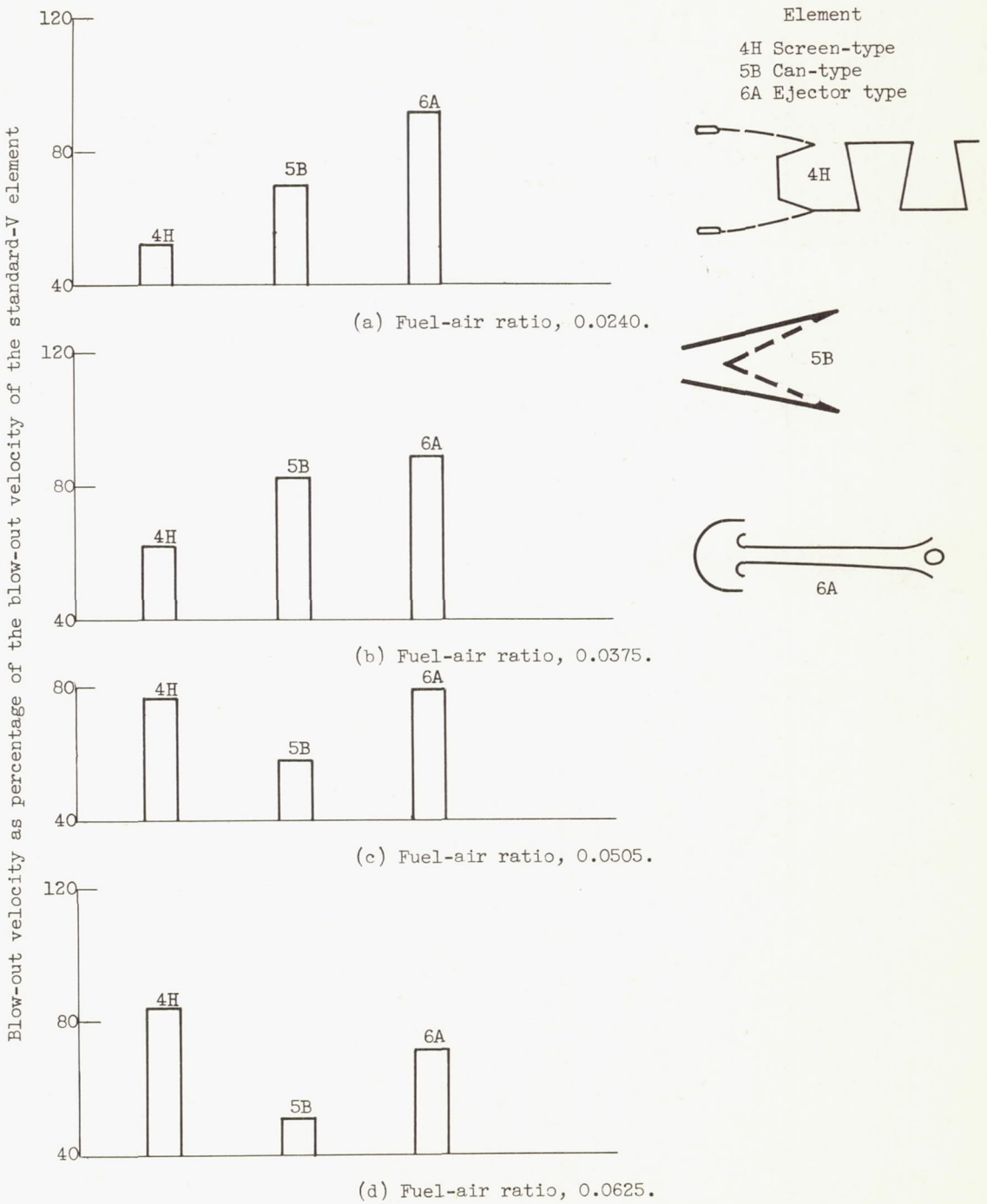

Figure 19. - Relative performance of several types of elements in assembly number 2.

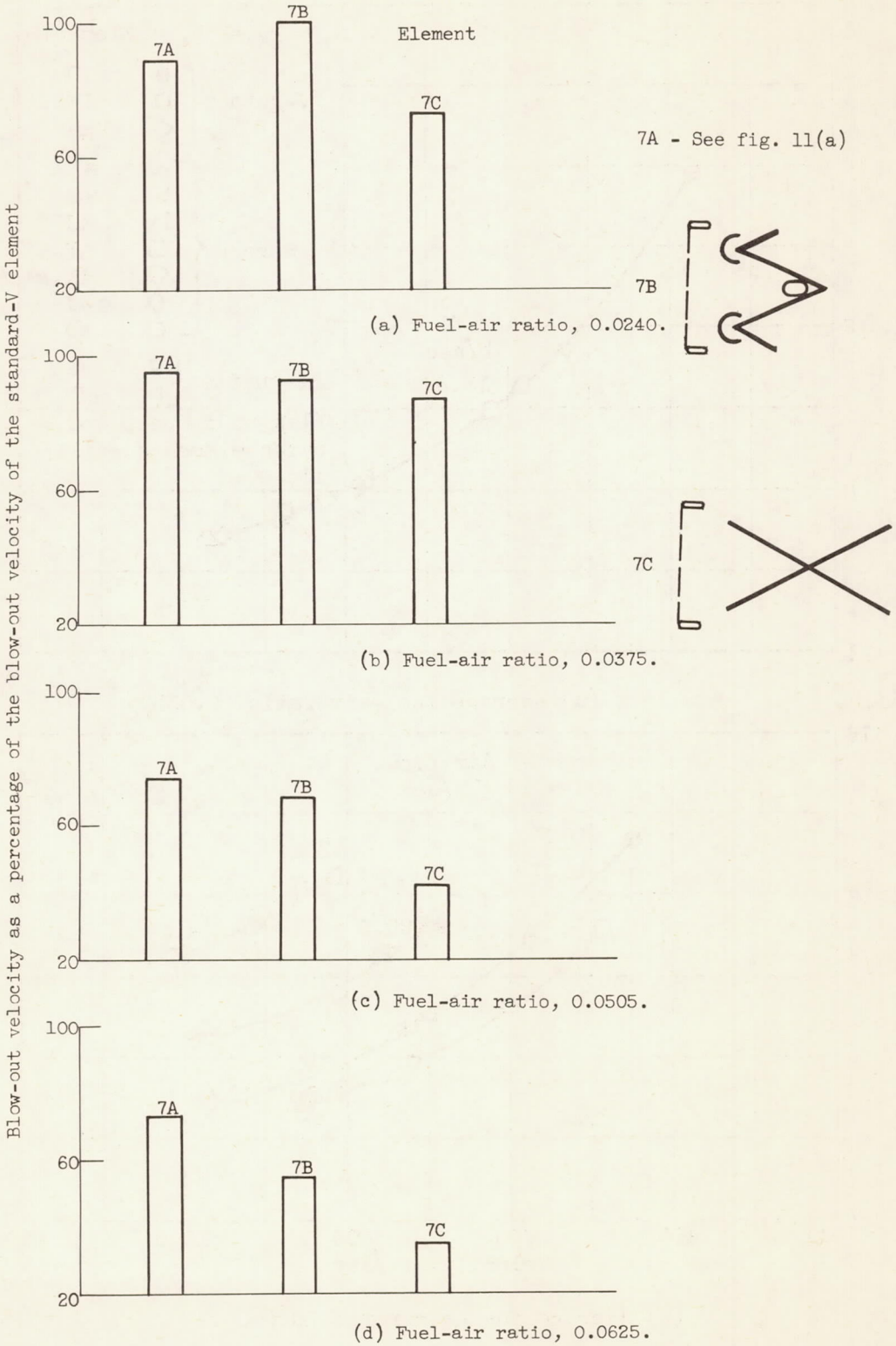

Figure 20. - Relative performance of several type 7 elements in assembly number 2.

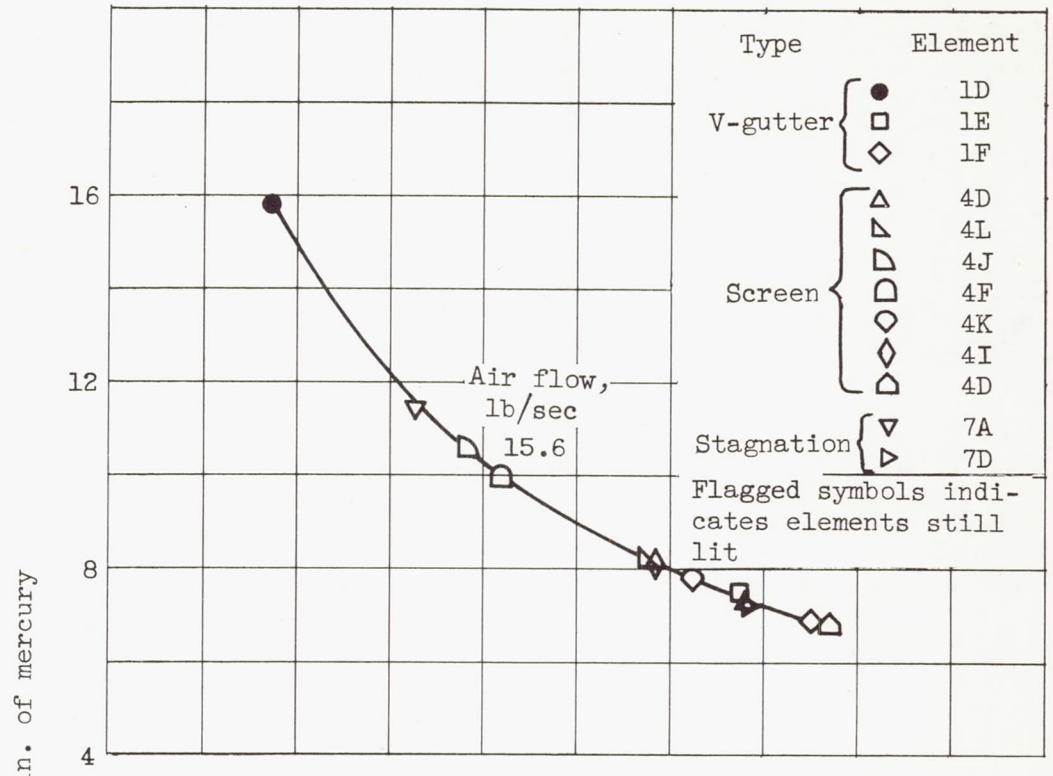

(a) Average fuel-air ratio, 0.035.

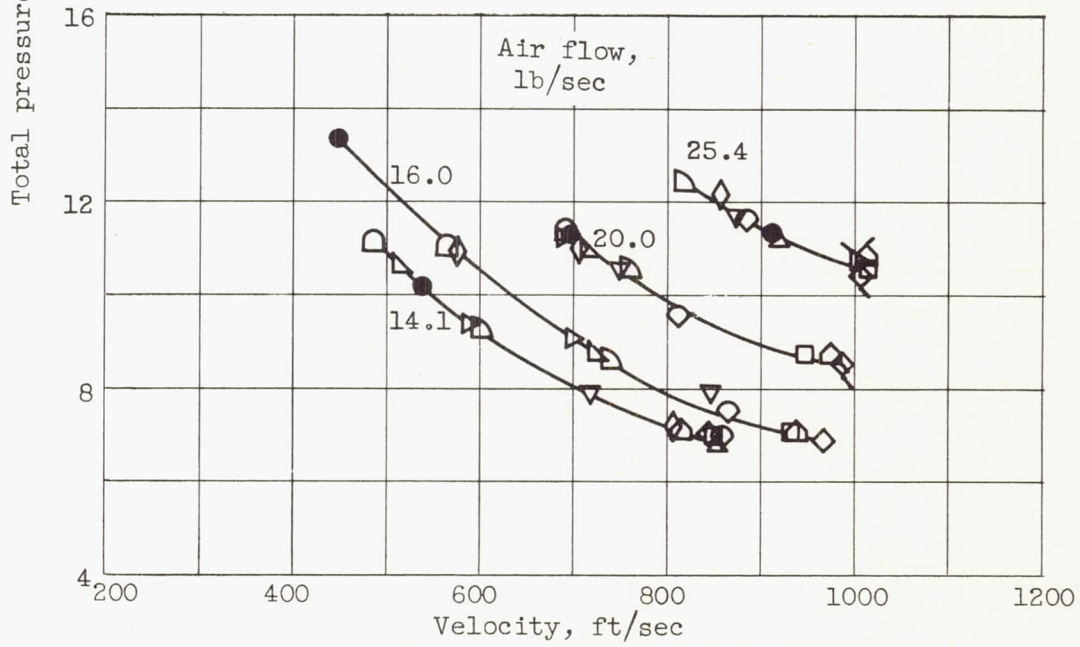

(b) Average fuel-air ratio, 0.0405.

Figure 21. - Stability limits of elements in number 3 assembly.

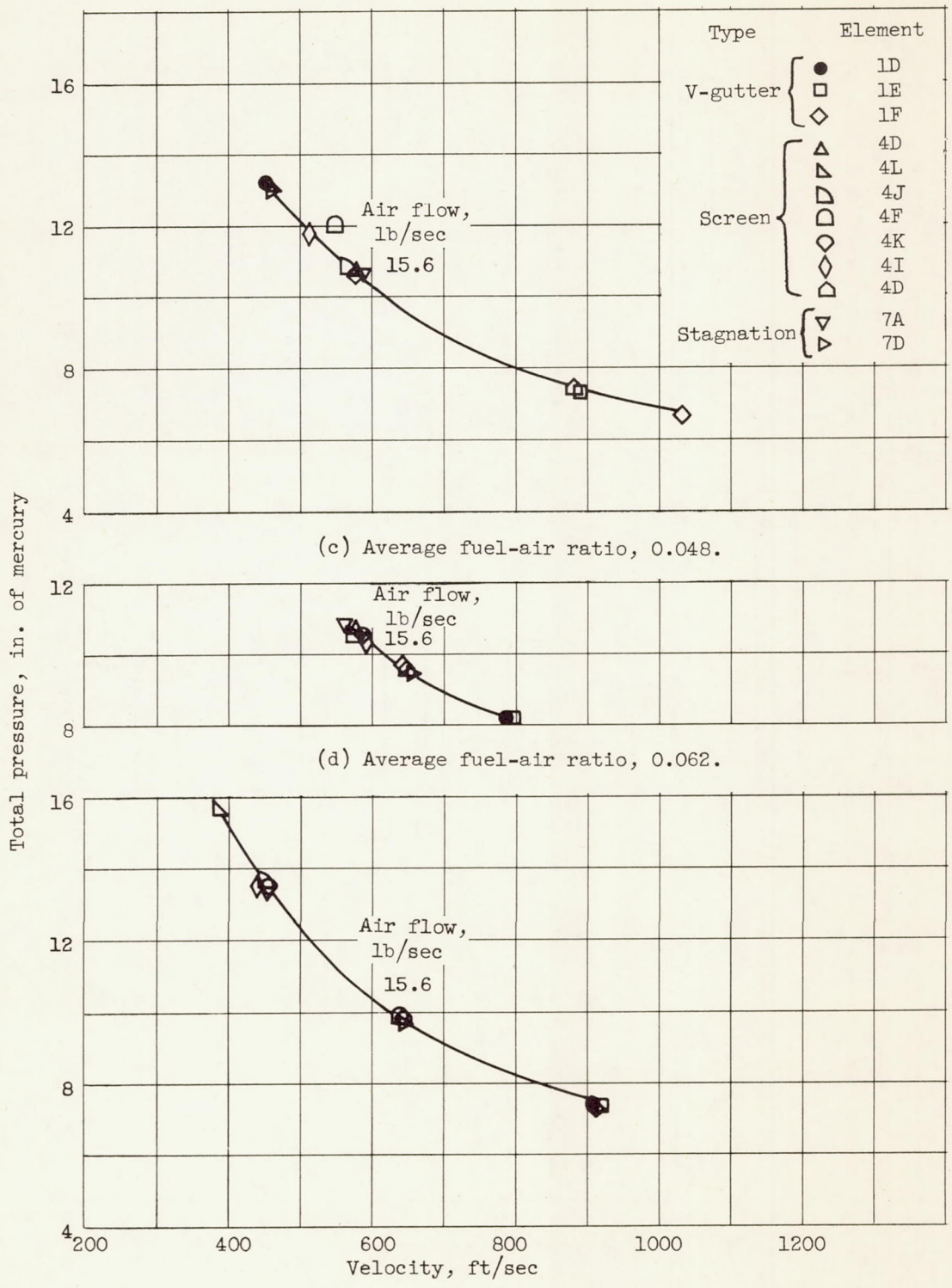

(c) Average fuel-air ratio, 0.048.

(d) Average fuel-air ratio, 0.062.

(e) Average fuel-air ratio, 0.0695.

Figure 21. - Concluded. Stability limits of elements in number 3 assembly.

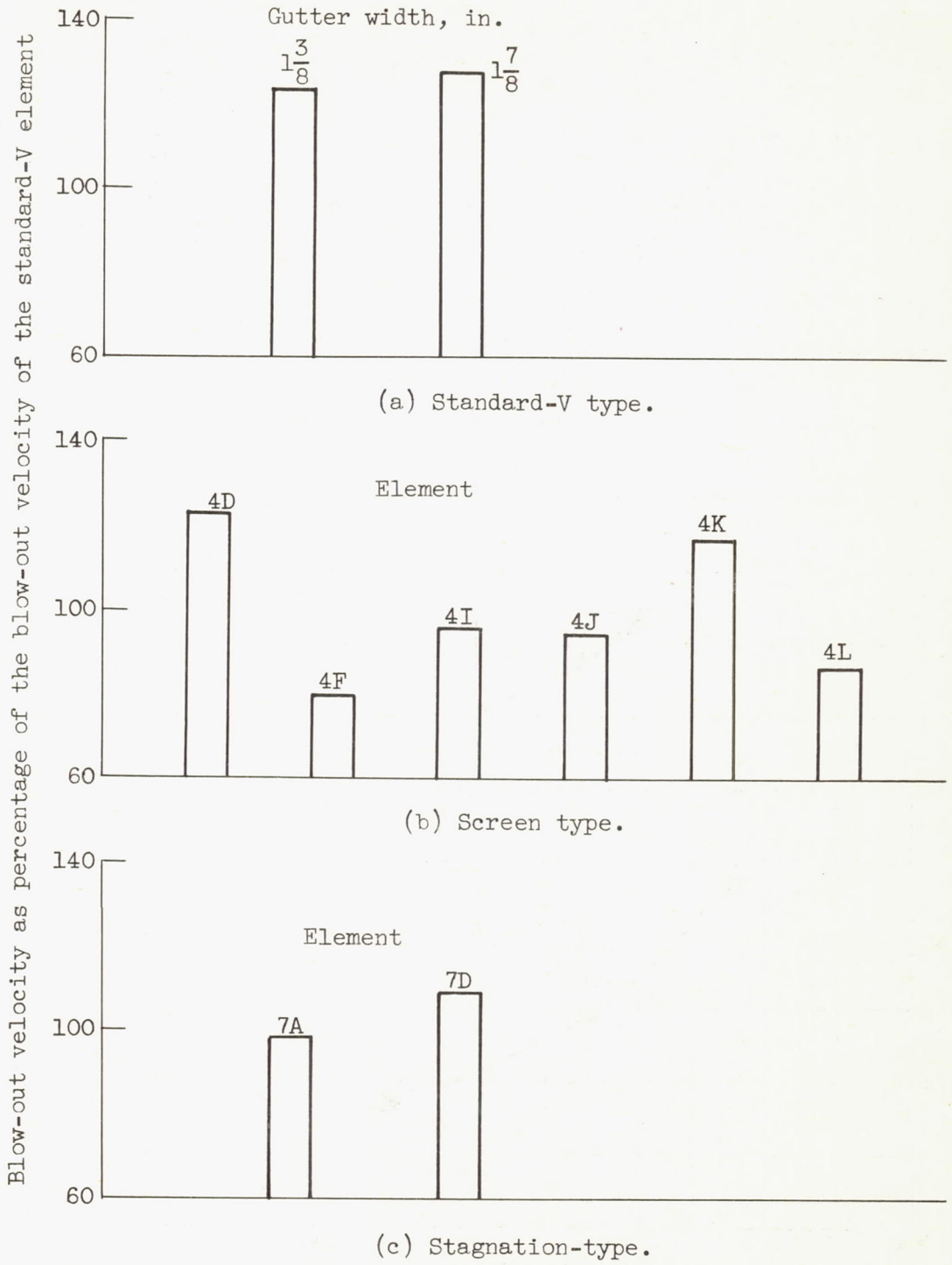

Figure 22. - Relative performance of elements in assembly number 3; fuel-air ratio, 0.0405.